SINTERING BEHAVIOUR OF COPPER COMPACTS OBTAINED FROM THE REDUCTION OF CUPROUS OXIDE PREFORMS

A Thesis Submitted
in Partial Fulfilment of the Requirements
for the Degree of
MASTER OF TECHNOLOGY

By
LALITESH CHANDRA

to the

DEPARTMENT OF METALLURGICAL ENGINEERING
INDIAN INSTITUTE OF TECHNOLOGY KANPUR
MARCH, 1991

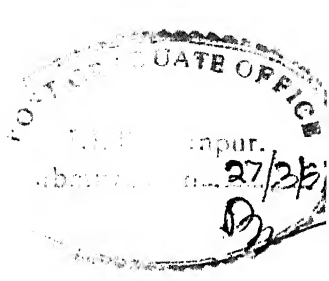

CERTIFICATE

It is certified that the work contained in the thesis entitled ' Sintering Behaviour of Copper Compacts Obtained from the Reduction of Cuprous Oxide Preforms', by 'LALITESH CHANDRA' has been carried out under our supervision and that this work has not been submitted elsewhere for a degree.

Dr. R.K. Dube
Professor
Dept. of Met. Engg.
I.I.T. Kanpur.

Dr. S. Bhargava
Assistant Professor
Dept. of Met. Engg.
I.I.T. Kanpur.

ACKNOWLEDGEMENTS

I owe my deep obligation to Dr. R.K. Dube and Dr. S. Bhargava for their valuable guidance, supervision, persistent encouragements, and informating discussion throughout the couse of this thesis.

I am thankful to Mr. S.C. Soni, Metal Working Laboratory for his overwhelming cooperation.

Finally, I wish to express my gratitude to my friends especially P. Ravi Kumar, R.K. Jindal, S.K. Singh and Atul Jain for their help and inspiration during my stat at I.I.T. Kanpur.

LALITESH CHANDRA

CONTENTS

LIST OF FIGURES

LIST OF TABLES

ABSTRACT

Sintering experiments were carried out on copper compacts formed by the reduction of cuprous oxide using hydrogen gas as the reductant, at three different reduction temperatures viz, 873K, 973K and 1073K for 5400 s. Sintering temperatures chosen were 1273K, 1173K and 1073K. Sintering of atomised copper powder samples were also carried out at the above temperatures, to compare the sintering behaviour of the two.

Results reveal that the density of copper compacts obtained from reduction of cuprous oxide preforms depends upon the reduction temperature. This was explained on the basis of morphological changes occuring during reduction at various temperatures. The difference in sintering behaviour of copper samples made by different routes is explained on the basis of defect concentration is the sample. After about a density of 3.8 gm/Cm^3, all types of copper compacts show similar rate of change in density.

CHAPTER - I

INTRODUCTION

Powder Metallurgy, like every modern technology began as an art. There are reasons to believe that it is the oldest kind of metallurgy and was practised before man was able to develop temperatures sufficiently high to melt metals. In India the use of fine powder of gold, silver, copper, and tin as paint materials can be traced to as early as AD 400-500.

Basically, there are two types of products which are made by powder metallurgy. The first type is ''sintered'' type, whèrein metal powder is compacted into the required shape followed by sintering at high temperatures. This type of product is characterised by the fact that it contains porosity ranging from 2-5% or even higher depending upon specific applications. The second type of product is known as ''sintered and worked'' type, wherein the product obtained after sintering are hot and cold worked to eliminate the porosity. Such products are also termed as '' P.M. Wrought products'' and have superior mechanical properties than just sintered products.

One of the most important process parameter controlling the economics of powder metallurgy processing is the sintering time. This is more pertinent in '' sintered'' type products, where porosity is eliminated by sintering alone. There have been consistent efforts to reduce the sintering time without affecting the quality of product.

1.1 Sintering of Metal Powder Compacts:

The term '' sintering '' is frequently used in a wrong and often misleading way. Powder Metallurgists often confuse sintering with the start of densification. Densification can no doubt be a criterion of sintering, however sintering can also occur without densification as in surface diffusion, lattice diffusion, and vapour transport. Based on a careful analysis of the sintering process a definition was proposed by Hausner (1) in 1963, as follows, '' sintering is the bonding of powders by molecular or atomic attraction in the solid state, by application of heat, causing strengthening of powder mass and possibly resulting in densification and recrystallization by transport of material''.

However, in the above definition, common and well established sintering phenomenon like liquid-phase sintering were not included. Thummler(1a), gave an improved definition, as follows, '' Sintering refers to aprocess of reducing the interior and exterior surface of a body or of bodies of particle in contact by reinforcement of contact bridges and the reduction of the void volume. During this process atleast one of the main components should be in the solid state''. Thus if there are two particles in contact with each other, sintering results in decrease of free surface area between the two by formation of neck. In a bulk semple, sintering also results in change in shape, size, number and volume of pores present because of this interparticle neck formation.

Studies indicate that material transport during sintering occurs through at least one of the following mechanisms (2) i) viscous flow, ii) plastic flow, iii) volume diffusion, iv) evaporation condensation and v) surface diffusion. Of these, evaporation condensation and surface diffusion can account for neck growth but not for the decrease in the distance between particle centres. Irrespective of the mechanism of material transport, surface free energy is the driving force for sintering. Thummler(1 characterized sintering as a three stage process. First stage is the rounding of pores resulting in strengthening of the powder mass and a decrease in electrical resistivity, but no change in the total pore volume and there for no change in density is observed. The second stage is characterized by the decrease in porosity i.e. decrease in total pore volume by decrease in the volume of some pores and total elimination of other pores. During this stage, densification occurs and grain growth starts. During third stage rapid grain growth occurs due to further decrease of porosity and perfect rounding of the pores.

Pines (2a) recognized that the concentration of the lattice vacancies (schottky defects) would be greater under concave pore surfaces than under a plane surface and concluded that the elimination of pores could occur by the diffusion of vacancies away from the pore in the resultant vacancy concentration gradient. Kuczynski (3) provided the quantitative proof of this by showing that to produce a neck of radius, x, should be related to the sintering time by an equation.

$$\left(\frac{x}{a}\right)^n = \frac{A(T)t}{a^m}$$

where a is the penticle radius, A(T) a function of temperature only and n and m are constants.

Sintering is normally carried out at temperatures in excess of 0.6 T_m At this temperature atomic mobility is high, diffusion processes are rapid and flow of material occurs at relatively low stresses. Inspite of these, the powder compacts retain porosity and take inordinately long time to attain a desired level of density coupled with required strength. Not only this, by conventional pressing and sintering quite often one gets i) lack in uniformity of strength along the dimensions of the specimen ii) lack inproperties such as elongation and impact resistance iii) require high temperature for sintering (as in W, Mo, Nb etc.). Further, certain compositions such as Fe-Si, Fe-Cr are difficult to homogenize by normal sintering procedure. The process of ' Activated Sintering ' offers the possibility of overcoming these difficulties by modifying the sintering atmosphere or metal powder surfaces.

1.2 Activated Sintering:

Sintering can also be defined as a diffusional creep under the action of capillary forces. This force, present at every curved interface between two phases is rather weak, therefore it is easily masked by the external forces which are usually stronger. The weakness of the capillary forces is the source of 'activity' because if the

force is feeble it must be very sensitive to the minute alteractions in a system of particles undergoing sintering. But as in the case of sintering, lot of confusion exists over defining 'Activated Sintering'.

'Activated Sintering ' is an expression (4) that has been used in connection with the sintering of powder compacts, where the rate of sintering is modified by some physical or chemical treatment of powder or compact or by incorporating reactive gases in sintering atmosphere with a view to enhance densification, mechanical strength, magnetic and electric properties. Shaler (5) after reviewing various aspects has suggested that one should fix adatum level and then with respect to it define ' Activated Sintering'. This now is the accepted convention to define activated sintering. Activated sintering mechanisms can be divided into three major classes (6).

1. Those which increase the sintering forces either by an increase of the surface or by an increase of the surface tension.

2. Those which accelerate the rate of theoretical perfect sintering, mainly the vacancy diffusion mechanism.

3. Those which create a new mechanism, either evaporation-condensation or surface diffusion.

Activation is sintering improves the physical properties of the sintered compact. This implies that sintering in more complete, that the porosity is less, or atleast that the pores are more spherical and therefore are less inimical to the physical properties. Application of

process rests upon the basic assumption that sintering is mainly a phenomenon connected with surfaces, and that therefore any activation of the surfaces of the powders or the pore structure of a compact must improve sintering ability.

Several physical and chemical methods of activation are now available. More common among them are (4) sintering in avarying magnetic field, sintering of mechanically deformed and irradiated specimens, sintering under static load (all physical methods) in - situ dissociation of hydrides, sintering under atmospheres containing a reactive gas, sintering in the presence of alloying elements, effect of prior oxidation of metal powder on the combined reduction and sintering etc.

Role of defect concentration for altering sintering kinetics is now well estabilished. Schatt and Friedrich (7) in 1985 showed that during sintering the material transport (densification) can be influenced by increased dislocation density under the action of capillary forces. Geguzin and co-workers (4a)using electrolytically deposited copper powder (having high internal stresses) could demonstrate a faster rate of shrinkage and an enhanced diffusion rate. By the creation of non-equilibrium concentrations of vacancies by irradiation with high energy particles it is possible to enhance diffusion processes. This is particularly true at lower temperatures, since at higher temperatures the additional vacancies anneal out and such irradiation has a very small effect on the diffusion

coefficient. Smoluchowski (8) working with NiO, showed that irradiating the oxide with protons before reduction considerably reduced the incubation time. This is presumably due to increased rates of diffusion.

The favourable effect of certain oxides which are reducible during the sintering of metal powders has been known for more than 35 years. The activation effect is manifested in densification, mechanical strength and electrical conductivity of the compacts. The favourable effect of oxides is observed in metals such as Fe, Ni, W, Mo, Cu, whose oxides can easily be reduced during the sintering process. The oxygen is introduced either as thin film of the oxide on each metal powder particle or it may be introduced in bulk form, e.g. mixture of metal and oxide powder.

Material transport primarily occurs by diffusion which may be

i) true bulk diffusion

ii) diffusion along dislocations

iii) surface diffusion

Diffusion along dislocation may be subdivided into 2(a) diffusion along the center of the dislocation, 2(b) diffusion in a cylinder around the dislocation (pipe diffusion) further surface diff.may be subdivided into 3(a) diffusion in the surface plane, 3(b) surface diffusion. Diffusion in crystals by either of the mechanisms 1,2(a) and 3(b) can take place when crystal defects are present (9).

Thus higher the defect concentration faster will be material transport i.e. an activated sintering. Point defects (vacancies) in the bulk of a crystal may arise in four ways

1) as a result of chemical reaction
2) as a result of suitable doping;
3) by irradiation with high energy particles or electromagnetic waves;
4) by plastic deformation

1.3 Mechanism of Activated Sintering:

The mechanisms of sintering of monometallic systems are not adequately understood. The conclusions based on model experiments and those derived from a study of the variation of physical parameters as a function of time and temperature are often contradictory. Several investigators are of the opinion that more than one mechanism operates during sintering. In a review on activated sintering, Shaler (5) attempted to explain the activation process by selecting a few pairs of systems which have been studied by various investigators. However, there are many difficulties in pinning down a definite mechanism for material transport during the process of activated sintering where several reversible and irreversible physico-chemical processes occur at the temperature of sintering.

In sintering where physical methods of activation are utilised and where diffusion processes are

responsible for material transport, vacancy concentration plays a decisive role. The increased non-equilibrium number of defects such as vacancies enhance the diffusion process. During the sintering of chemically activated systems either the modification of the surface configuration of the particles in the presence of reactive gases, or the scavenging of reactive gas yielding a highly active surface, or the formation of solid solution giving phases with enhanced chemical reactivity in nascent state, or the reduction of oxides giving rise to highly active metallic atoms is responsible for faster material transport.

1.4 Reduction of Cuprous Oxide:

As pointed out above that an oxide can activate the sintering kinetics only when it is reducible during reduction. In this light it becomes imperating to understand the reduction mechanism of metal oxide. Since our present study is only related with copper oxides, only copper oxide reduction is being dealt with in detail. Most copper metal powders manufactured by reduction of oxides are produced by using either solid carbon or gases like hydrogen, carbon monoxide, or mixtures of such gases.

Ellwood and Weddle (10) studied the reduction of copper oxides by various gases. The reducing media investigated were hydrogen, carbon monoxide, cracked ammonia, coal gas and propane. The economic advantage was the reason for investigating the suitability of cracked ammonia, coal gas and propane whereas hydrogen and carbon

monoxide were used not only because they are good reducing agents but also because of their different mechanism of reduction. In hydrogen reduction the process is essentially one of diffusion of the gas into the particles, so that internal reduction occurs, with the possibility of steam being trapped in the particles. The reduction is preceded by an incubation period, the length of which is greater at lower temperatures. Following the incubation period, (during which there is no perceptible reaction) reduction sets in at a steadily increasing rate (induction period) till a maximum is reached, after which the rate decreases gradually to zero as the reaction approaches completion.

Some well-known facts are :

a) Oxygen has a small solubility in copper;

b) Oxygen and cuprous ~~oxide~~ ions can readily and quickly diffuse within solid copper;,

c) hydrogen readily diffuses in solid copper but H_2O and CO do not.

The equilibrium data of the reaction $Cu_2O+H_2 \longrightarrow 2Cu+ H_2O$ indicates that the reduction is an exothermic reaction. The exothermic heat is dissipated by

i) conduction heat transfer within the strip, i.e. to the porous copper product layer and the unreduced layer of cuprous oxide.

ii)Conduction heat transfer to the boundary gas film surrounding the strip to the cooler reactant gas flowing over the gas.

iii) natural convection of heat through the gases flowing into the pores of the strip.

iv) radiative heat transfer to the cooler surroundings in the reaction chamber.

Considerable heat is evolved during early stages of the reaction, the rate of reduction being maximum. H_2 gas readily diffuses into copper. Since the H_2O formed by reaction with oxide cannot readily diffuse out, it must either blow its way out, forming internal cavities, or escape through fissures (11). This largely explains the fact that a copper powder made through oxide reduction is quite porous or spongy. The reduction of the preformed copper oxide strip involves the following steps (12), and a similar mechanism would also be valid for the reduction of small size copper oxide compacts.

(i) external mass transport of hydrogen from the gas delivery system to the outside surface of the oxide strip.

(ii) diffusion of hydrogen within the pores of the strip.

(iii) Chemical reaction at the reaction interface.

(iv) out ward diffusion of gaseous H_2O, formed during the reaction, through the pores of the strip.

(v) mass transfer of gaseous H_2O into the bulk stream.

Solid state reduction of cuprous oxide (Cu_2O) shows a nucleation and growth type of mechanism. Hydrogen on coming in contact with cuprous oxide surface nucleates copper at a few energetically favourable points. During the subsequent stages of the reduction, the copper nucleates and grows at more points and slowly covers the entire surface. After the entire surface has been covered with the first layer of reduced copper, further penetration of hydrogen to the copper/cuprous oxide interface occurs by diffusion through the newly formed pore channels in between the different copper islands. When hydrogen becomes available at the next reaction interface, further nucleation of copper occurs. Thus the reduction proceeds outwards from the nuclei, particle to particle. As the reaction interface penetrates towards the centre of particle, the outermost shell of copper is subjected to continuous heating as a result of the dissipation through it of the exothermic heat which promotes sintering between islands of copper.

1.5 Effect of Reduction Temperature and Time on Particle Size and Internal Strain :

Not much information about the effect of reduction temperature and time on particle size and Internal

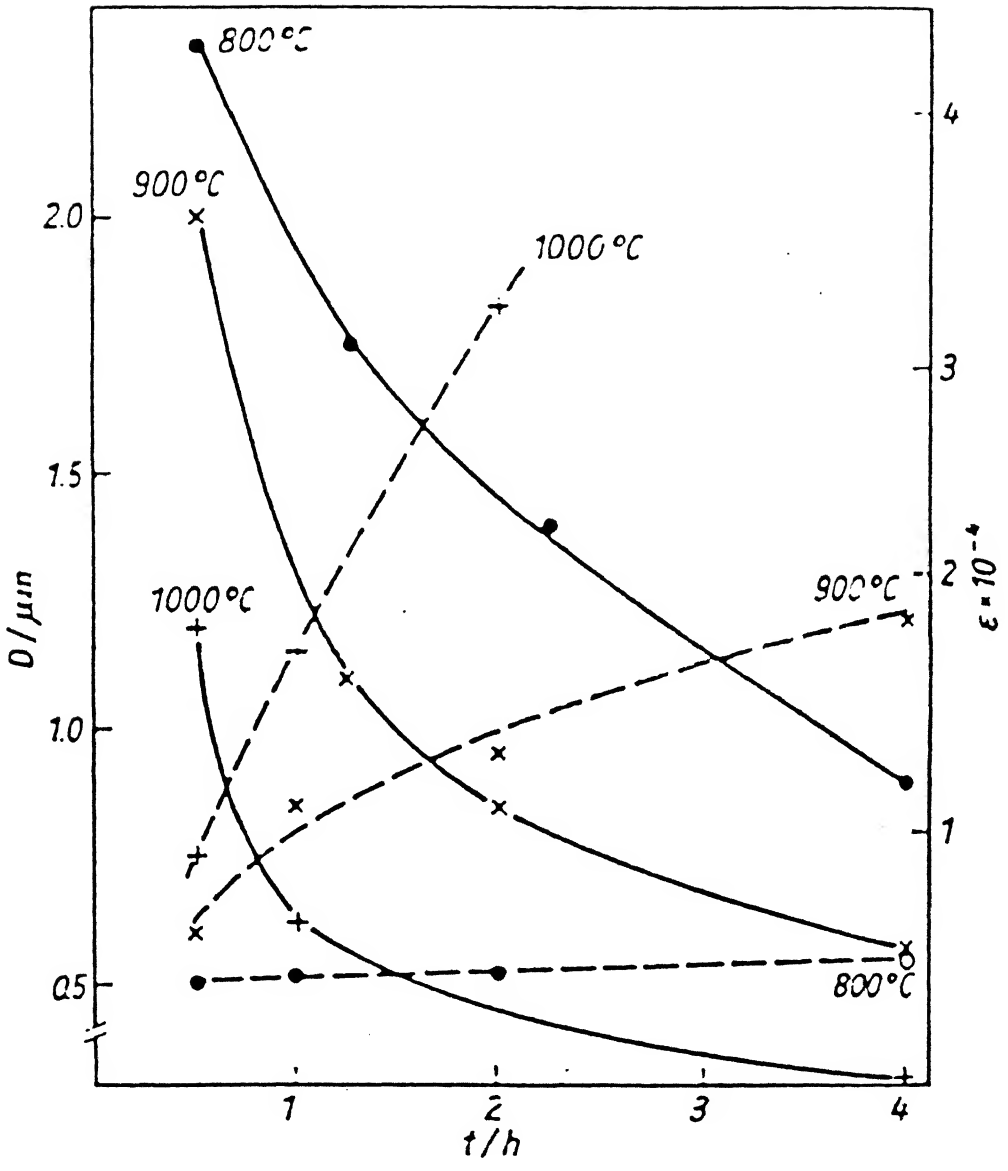

Fig. 1.1 Influence of reduction temperature and time on particle size and internal strain of tungsten powders (2. reduction step). - - - - D, ——— ε

strain is available. However, Salewski (13) working with tungsten oxides (WO_3 or $W_{20}O_{58}$) has shown that internal strain (a measurs of internal defect concentration) decreases whereas the particle size increases with increasing temperature of reduction (Fig. 1.1) . The decrease in internal strain with reduction time was because of annealing effect. Annealing effect also results in an increase in particle size.

CHAPTER - II

OBJECTIVE AND SCOPE OF THE STUDY

The present investigation on the study of the sintering behaviour of copper compacts obtained from the reduction of cuprous oxide preforms has the following objectives:

(i) To study the sintering behaviour of reduced copper compacts obtained after reduction of cuprous oxide preforms at different temperatures.

(ii) To study the microstructural features of (a) as -reduced (b) as-reduced followed by sintering, of copper samples.

(iii) To compare the sintering behaviour of reduced copper compacts with those of atomised copper powder.

CHAPTER -III

EXPERIMENTAL PROCEDURE

3.1 Raw Materials:

3.1.1 Cuprous Oxide:

Analytical reagent grade cuprous oxide powder supplied by central Drug House (P) Ltd, Delhi was used in the present investigation. Important characteristic provided are as follows:

Cu_2O content - 94% (Min.)
CuO content - 5% (Max.)

In order to estimate the particle size of the supplied powder sieve analysis on the as-supplied powder was done. Results of the sieve analysis are shown in Table 3.1.

Since surface topology of the oxide powder play an important role in determining the morphology of copper powder produced by its reduction, an examination of particle shape and topology of cuprous oxide was carried out by SEM. Prior to examination under SEM, cuprous oxide powder particles were given a silver coating to avoid accumulation of electrical charge, since cuprous oxide is non-conducting.

Typical particle shapes and surface topology of Cu_2O powder is shown in Figure 3.1(a) and 3.1(b) which show that Cu_2O particles are highly porous and spongy.

TABLE 3.1

Particle Size Distribution of Cuprous Oxide Powder Particle.

Mesh Size	+100	+200	-200
µm Size	+150 µm	+75 µm	-75 µm
Percent	81	19	0

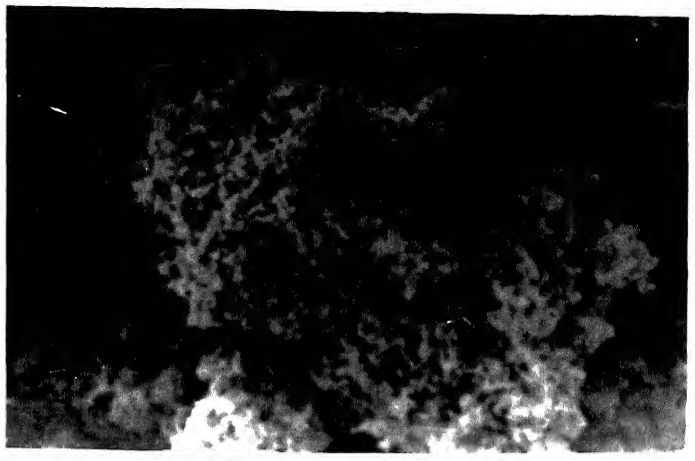

(a) 350 X

(b) 3500 X

Fig. 3.1 Typical particle shape and surface topology of Cu_2O particle (a) 350 X (b) 3500 X.

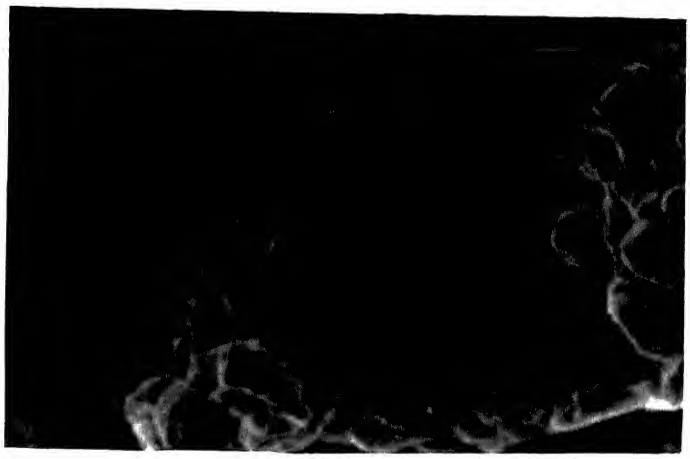

(a) 1250 X

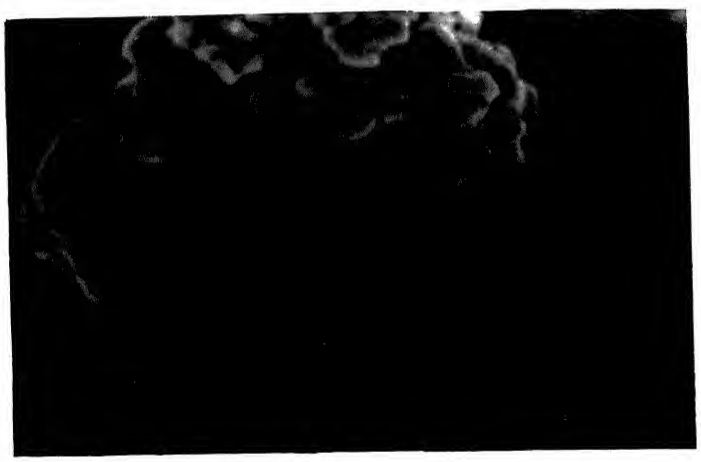

(b) 2500 X

Fig. 3.2 Typical particle shapes and surface topology of atomised copper particle (a) 1250X (b) 2500 X.

3.1.2 Atomised Copper:

Atomised copper powder supplied by Green Back Industries Inc., U.S.A. was used to compare its sintering behaviour with those of reduced copper. Important characteristics provided are as follows:

Cu content - 99.5%

Powder size - 63.9% of - 325 mesh.

Apparent density- 2.83 kg/m^3

Hall flow meter rating - 3.45 / 50 gms.

Typical particle shapes and surface topology of Cu_2O powder is shown in Figure 3.2(a) and 3.2(b) . It can be seen that atomised copper particles have folds and porosity.

3.1.3 Methyl Cellulose:

Reagent grade methyl cellulose powder supplied by Loba Chemie Indo Australia Co. was used as a binder in slurry casting.

3.2 Making of Cuprous Oxide Preforms:

Reduction of cuprous oxide by hydrogen gas to obtain copper can be carried out by three different methods, as follows :

(i) Fluidized bed reduction

(ii) Reduction of pressure compacted samples

(iii) Slurry casting

Reduction of cuprous oxide particles while suspended in an upward stream of gas, as in fluidized bed reduction has till now not been studied and therefore is in itself an area of investigation. Moreover, even if one gets isolated reduced copper by fluidized bed reduction, further processing will require its shaping by either of the other two methods. This method was therefore not pursued.

Reduction of pressure compacted samples can be carried out easily. However, reduction reaction of cuprous oxide is highly exothermic and is associated with H_2O vapour formation. Dissipation of heat by conduction and diffusion of gaseous H_2O through pore channels is difficult because of high density of compacts produced by pressure compaction technique. This results in excessive cracking and lamination formation when such a sample is reduced with hydrogen. This was verified by making die-compacted cuprous oxide samples using a pressure just sufficient to get a pallet with sufficient handling strength. These pallets when reduced at 873K ($600^{\circ}C$) under hydrogen atmosphere did result in samples with excessive lamination formation and creacking. This method was also therefore not pursued with.

Slurry casting, is a process which consists of a sustained suspension of particles, with the chemical circumstances so arranged that the particles are prevented

SLURRY COMPOSITION

Powder	-	59.0%
Methyl Cellulose	-	0.6 %
Water	-	40.4 %

from aggregating or floculating. Slurries are usually poured into a suitable mould and is quickly dried. This results in green strip which is porous in which particles are not cold worked or deformed. The particles therefore have point contacts with each other with sufficient porosity to allow easy dissipation of exothermic heat and diffusion of gaseous H_2O . With this in view, slurry casting was chosen as a method of preform making throughout the present study.

The slurry was made by mixing methyl cellulose and metal powder in distilled water. The agglomerates of powders formed was broken by stirring the entire mixture with a mechanical strirrer till a homogeneous slurry with good flow characteristics was obtained. This slurry was poured into flat horizontal steel mould of size 100 X 75 X 5 mm. Before pouring the slurry the mould surface was coated with oelic acid for facilitating with drawl of dried strip. The cast slurry was dried by heating the mould on a hot plate. In order to avoid overheating, the strip was released from the mould before it was fully dried and was further dried in the oven at 383 K ($110^{o}C$) for 1800s (30 min.). A coherent cuprous oxide strip so formed had the dimensions of 95.1 X 70 X 4.: mm and that for atmoised copper powder strip was 90.7 X 68.5 X 4.1 mm. Each strip was cut with a surgical blade into twenty smaller ractangles of almost

similar sizes. Some strips of atomised copper powder by using the above method were made to compare its sintering behaviour with those of reduced copper samples.

3.3 Reduction of Cuprous Oxide Preforms with Hydrogen:

Reduction reaction of cuprous oxide preforms was carried out in a specially designed tube furnace. The reduction chamber, which was heated by silicon carbide rods, consisted of an Inconel tube closed at one end. The open end of the furnace had a 250 mm long cooling chamber, where the reduced copper samples were cooled for 1800 s (30 min.) to a temperature of about 373K ($100^{o}C$) under hydrogen atmosphere prior to taking them out of the furnace. The gases were introduced at the bottom side of the closed end of the furnace tube from a steel tube. The unused reducing gas was burnt at the exit.

The standard procedure for the reduction was that the furnace temperature already maintained at the required temperature, was flushed with nitrogen for about 600 s (10 min.). Then hydrogen was introduced and the nitrogen flow was stopped. A hydrogen flow rate of 6.67×10^{-5} m^3/s was maintained through out the reduction operation. The green cuprous oxide preforms were placed on a perforated steel strip and then pushed into the hot zone of the furnace. The preforms were kept under these conditions for 5400 s (90 min.) and then withdrawn to the cooling chamber. The reduced copper samples were cooled for

1800 s (30 min.) and then taken out of the furnace. Cooling was necessary to avoid excessive oxidation of reduced copper samples. The samples were always kept in a decicator under a vacuum of 20 μm Hg to avoid any oxidation. The samples were taken out of the decicator only for the purpose of density measurement or for sintering. The reduction temperatures chosen for the present study were 873K (600°C), 973K (700°C) and 1073K (800°C). As pointed out earlier, the reduction temperatures and the time of reduction were so chosen, so as to ensure 100% reduction of cuprous oxide particles.

In cases where a study of morphological changes occuring during the reduction reaction was to be done, the preforms were partially reduced at 1073K (800°C) for 90 s (1.5 min.) under a hydrogen flow rate of $3.33 \times 10^{-5} m^3/s$. After partial reduction the preforms were cooled in hydrogen atmosphere for 1800 s (30 min.).

3.4 Sintering of As-Reduced Copper and Atomized Copper Samples:

Sintering of as-reduced coper samples was carried out in the furnance used for the reduction of cuprous oxide preforms. A hydrogen flow rate of 6.67×10^{-5} m^3/s was maintained throughout the sintering and cooling steps. The as-reduced copper samples were sintered at the temperatures of 1273K (1000°C), 1173K (900°C) and 1073K (800°C). Once the required

furnace temperature was attained, the nitrogen gas was passed to flush air out of the reaction chamber and then hydrogen gas was passed and ignited at the exit. Three samples of each reduced at 873K (600°C) , 973K (700°C) and 1073K (800°C) along with the samples of atomised copper was placed on the perforated steel tray and pushed into the hot zone of the furnace. The tray was withdrawn into the cooling zone after a predecided time period had elapsed. The sintered sample were kept in cooling chamber for 1800 s (30 min.) and then were withdrawn for density measurements by impregnation technique. The sintering time allowed in most cases was 300 s (5 min.), 900 s (15 min.), 1800 s (30 min.), 3600 s (60 min) and 720C s (120 min.). However, for sample reduced and roll-compacted a schedule of 180 s (3 min.), 720 s (12 min.), 1200 s (20 min.), 3000 s (50 min.) and 6000 s (100 min.) was followed.

3.5 Compaction of As-Reduced Copper Samples and Their Sintering:

Density of copper sample obtained by cuprous oxide reduction at different temperatures, was different, Sintering behaviour of any powder preform being dependent on the arrangement of particles in the preform, a differing in initial density may have affected the sintering behaviour . The samples with lower densities were cold rolled in a rolling mill with the following specifications:

Roll radius	- 67.5 mm
Roll speed	- 508.68 mm/s
Horse power	- 7.8

The rolls were not lubricated. The compaction done was only to achieve a particle rearrangement for increasing density. Previous work on compaction of reduced copper samples (14) show that no cold working or deformation occurs upto 45% compaction. Any cold working of particles would have affected the sintering behaviour. Therefore the maximum reduction given was kept below this level. For copper samples obtained by cuprous oxide reduction at 873K (600^{o}C) were given 43% compaction whereas atomised copper samples were given 40% compaction with respect to initial thickness.

3.6 Methods of Testing and Inspection:

Sintering is a process of reducing the interior and exterior surface of body or of bodies of particle in contact by reinforcement of contact bridges and the reduction of the void volume. Thus sintering, besides resulting in the decrease of free surface area between the particles by the formation of necks, it also results in change in shape, size, number and volume of pores and hence change in density of powder mass. Therefore, the methods of testing and inspection suitable to study these were chosen.

3.6.1 Density Measurement:

The density of the green atomised copper strip was calculated from weight and dimension measurements. Densities of the sponge copper strips and that of the further densified strips were determined by the immersion technique. Reagent grade ethylene glycol was used for impregnating the samples. Ethylene glycol was chosen because it has a lower vapour pressure, compared to that of water, and therefore does not start boiling when entrapped air is pulled out from the samples under vacuum.

The samples, immersed in glycol, were placed in a vacuum decicator and the pressure was reduced to 20 μm Hg. This enabled the entrapped air to come out through the open pores. By repeating the process of creating the vacuum 3-4 times it was possible to remove almost all the air from the samples. These open pores were inturn filled with glycol. The surface film of glycol over the inpregnated samples was removed by wiping the samples on a sponge. The following relationship was used to calculate the density of sinter-

$$\rho_s = \frac{W_1}{W_2 - W_3} \rho_f \qquad \ldots (3.1)$$

where,

ρ_s = density of sinter

W_1 = weight of sample in air

W_2 = weight of sample in air after impregnation with glycol

W_3 = weight of the impregnated sample in glycol

ρ_f = density of ethylene glycol.

3.6.2 Metallography:

Sintering being closely linked with the changes in external as well as internal surfaces, a study of these using optical and scanning electron microscope was done.

(i) Optical Microscopy:

Study of internal surfaces, size, and shape and number of intra-particle pores was done using an optical microscope. Any direct polishing method could not be employed for porous samples because these being soft and ductile will undergo particle erosion and not particle polishing . Therefore it was necessary to impregnate the pores with epoxy resin which could be cured subsequently. A mixture of Araldite expoxy resion and hardner in the proportion of 10:1, by weight was used for this purpose.

The polishing procedure adopted was standard. The epoxy impregnated samples were polished in the following sequence-

Belt polishing ⟶ emery papers starting with 0/0 to 4/0 through 1/0, 2/0 and 3/0 ⟶ Final polishing on a microcloth wheel using a 0.05 μm alumina water slurry.

After final polishing the specimens were washed with water, dried and etched with NH_4OH-H_2O_2 solution. After etching they were rinsed with running tap water and dried under a warm air blast.

(ii) Scanning Electron Microscopy:

The fractured surface of the reduced copper strip sintered at various temperatures was also examined with JOEL make scanning electron microscope. The cuprous oxide powder and atomised coper powder had to be coated with a silver film to avoid accumulation of changes in the powders.

3.7 Curve Fitting:

The equation for variation of density as a function of time was desired for further analysis regarding rate of change of density ($\frac{\partial \rho}{\partial t}$) and the parameter $\frac{\partial}{\partial t}(\frac{\partial \rho}{\partial t})$.

A best fit curve was found using GRAPHER package on IBM PC XT. The experimentally obtained values were fed and was approximated with one of the five type of best fit equations available. The available options were linear, logarithmic, exponential power law and cubic spline. By hit and trial the best fit equation type from the these available options was noted for further analysis.

CHAPTER - IV

EXPERIMENTAL RESULTS

4.1 Solid State Chemical Reaction of Cuprous Oxide Preforms:

Solid state reduction of cuprous oxide preforms was carried out by reacting them with hydrogen at three different temperatures viz. 873K (600°C), 973K (700°C) and 1073K (800°C) by maintaining a gas flow rate of 6.68×10^{-5} m^3/s for 5400 s (90 min.). Previous investigation (14) on the solid state reduction of cuprous oxide compacts using H_2 as a reductant suggest that the reduction of cuprous oxide occurs very rapidly. For example, almost complete reduction of cuprous oxide compacts of thickness 4.8 mm of density 2.3 g/ Cm^3 was obtained by reducing at 1073K for obout 1200 s using the flow rate of hydrogen as used in the present study. However, some occluded oxide particles at the core of reduced copper mass was observed. Further heating under hydrogen atmosphere was required to reduce them completely. Therefore, in order to have 100% reduction of Cu_2O a higher reduction time of 5400 s (90 min) was used in the present investigation.

4.1.1 Variation of Density of Reduced Copper Specimen with the Reduction Temperature:

Density of copper samples obtained by the reduction of Cu_2O preforms for 5400 s (90 min.) was found

to vary with the temperature of reduction. Table 4.1 shows the variation of density and relative density of oxide reduced copper with the reduction temperature. It can be seen that the density of reduced copper samples increases with increase in the temperature of reduction.

4.1.2 Morphology of Reduced Copper Samples:

Sintering behaviour of any powder preform is intimately linked with the arrangement of particles in the preform, total surface area per particle and concentration of defects and their diffusivities. In order to study the arrangement of particles and their morphology in copper sample formed by reduction of Cu_2O preforms, optical and as well as scanning electron microscopy were carried out.

SEM examination of fractured surface of reduced copper samples was carried out Fig. 4.1(a), 4.1(b) and 4.1(c) show the typical SEM micrograph of copper sample reduced at 873K (600°C) and 1073K (800°C) respectively, In order to understand the formation of copper phase the fractured surface of partially reduced cuprous oxides were examined under SEM.

Fig. 4.2(a) and 4.2(b) show the fractured surface of cuprous oxide preforms reduced at 1073K (800°C) for 90 s(1.5 min.). Similar technique has been used earlier to study the morphological changes occuring during the reduction of iron oxide and Cu_2O. It can be seen from the

TABLE 4.1

Variation of Density and Relative Density of Oxide Reduced Copper with the Reduction Temperatures .

Reduction Temperature	Density gm/Cm^3	Relative Density
873K	1.98-2.1	0.22-0.23
973K	2.63-2.91	0.29-0.32
1073K	3.23-3.49	0.36-0.39

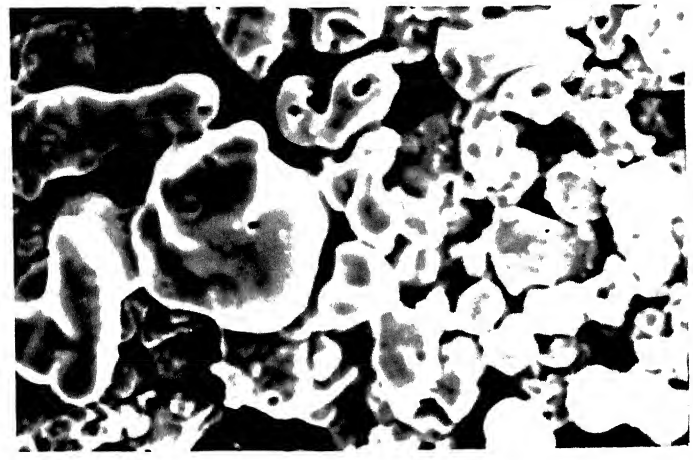

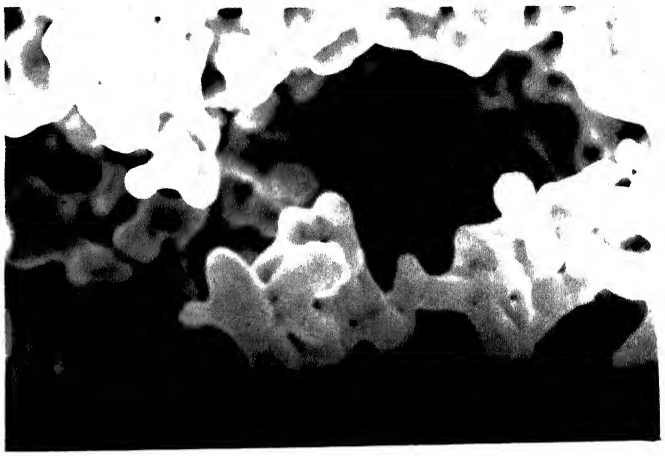

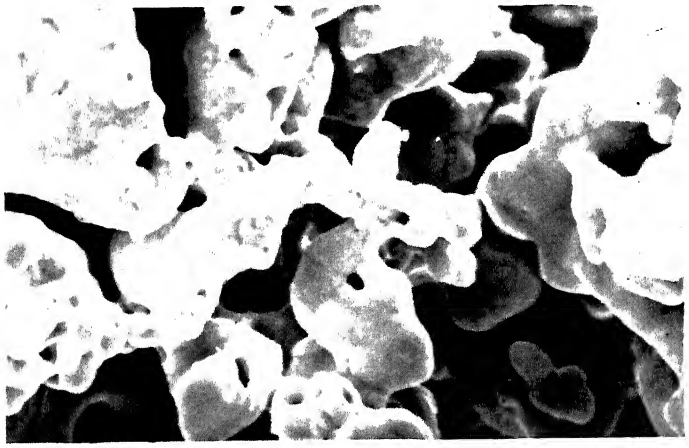

Fig. 4.1 SEM micrographs of reduced copper showing pore morphology (a) and (b) reduced at 873K (c) reduced at 1073K for 5400 s.

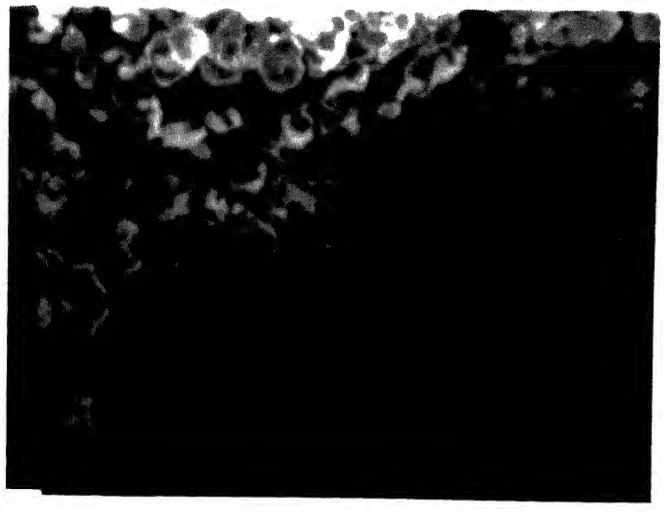

(a) 1500X

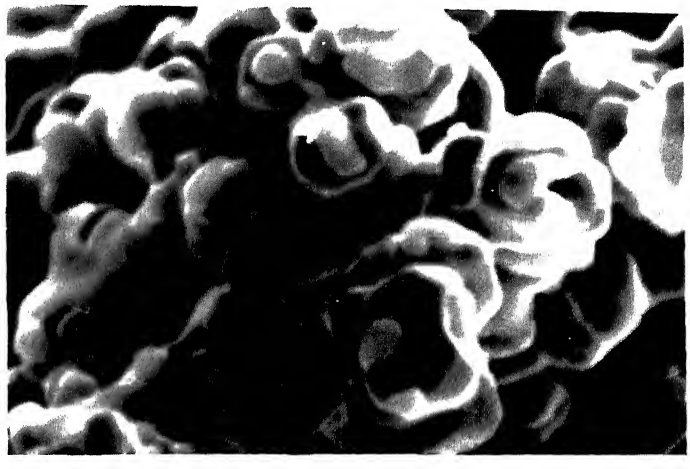

(b) 5000X

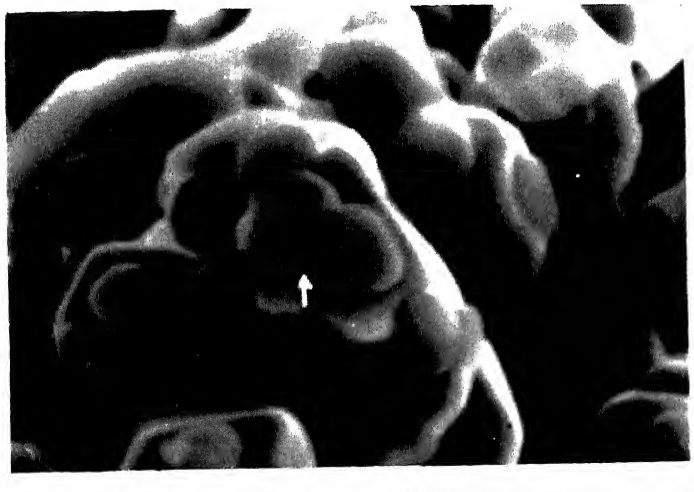

(c) 9000X

Fig. 4.2 SEM micrograph of partially reduced cuprous oxide particle at 1073K for 90 s (a) and (b) nucleated islands of Cu (c) sintering of nucleated Cu islands.

above figures that semi-spherical copper islands have nucleated and grown on parent Cu_2O particle surface as shown by arrow mark in Fig. 4.2(b). With the progress of reduction such copper islands form at more locations and subsequently start getting sintered with each other as shown in Fig. 4.2(c) marked by an arrow. After complete reduction, reduced copper would consist of large number of copper grains formed by nucleation and growth process and simultaneously sintered with each other during the course of reduction.

From Fig. 4.1(a) to 4.1(c) it can be observed that the sintering between various nucleated and grown copper island is comparatively less in samples reduced at 873K (600°C) than at 1073K (800°C) . This observation explains the difference in densities obtained after reducing the cuprous oxide samples at different temperatures for same period of time as shown in Table 4.1. Further, it can be seen that in case of copper samples reduced at 873K, although in certain regions several neighbouring islands sintered together to form a bigger conglomerate of islands, but by and large most of the conglomerates are smaller in size than those in samples reduced at 1073K (800°C). In both the cases because of sintering, the surfaces of conglomerates/islands were smooth.

The etched microstructure of copper samples reduced at 1073K (800°C) and 873K (600°C) are shown in Fig. 4.3 and 4.4 respectively. It can be seen that

200X

Fig. 4.3 Etched microstructure of copper sample reduced at 1073K.

200X

Fig. 4.4 Etched microstructure of copper sample reduced at 873K.

annealing twins are present in the samples reduced at 1073K (800°C) while the sample, reduced at 873K (600°C) did not show such twins. The presence of annealing twins in samples reduced at 1073K (800°C) and their absence in those reduced at 873K(600°C) indicates that the exothermic heat evolved during reduction at 1073K (800°C) indeed is very high.

4.2 Sintering Behaviour of As-Reduced Copper Specimen:

Copper samples formed by reduction with hydrogen at 873K (600°C), 973K (700°C) and 1073K (800°C) were sintered at 1073K (800°C) , 1173K (900°C) and 1273K (1000°C). Two phenomena that occur during sintering are reduction in total porosity, or densification caused by the increased contact area between particles and smoothening of internal surfaces of the pores. Therefore sintering behaviour of any powder sample should be dependent on the arrangement of particles in the sample, total surface area per particle and concentration of defects and their diffusivities. Thus a study of sintering behaviour in terms of variation in density and total contact area per particle as a function sintering time and temperature becomes imperative. A limited amount of study on sintering behaviour of compacts prepared from atomised copper powder was also carried out to compare the sintering characteristics of reduced copper with it.

4.2.1 Variation of Sintered Density with Sintering Time and Temperature:

Densification occuring during sintering may take place by several mechanisms of transport from various solid parts by the sample towards the pores. Temperature of sintering is found to affect densification behaviour. Raising the temperature increases the rate of densification and also has a higher value of final density obtained after any given period of time (Fig. 4.5). As pointed out earlier, at lower temperatures of reduction the sintering between freshly formed copper nuclei and between two particles is less. Therefore, the copper particle thus formed by oxide reduction will contain more intra-particle and inter-particle porosity. Further, it is also expected to contain a higher concentration of defects than those reduced at higher temperature. This is because the exothermic heat evolved at higher temperatures of reduction is considerable and therefore annealing of copper formed occurs.

The variation in sintered density as a function of sintering time and temperature of reduction is shown in Figure 4.6(a),4.6(b)and 4.6(c) for reduced copper samples sintered at 1273K (1000^{o}C), 1173K (900^{o}C) and 1073K(800^{o}C) , respectively. Three distinct regions: initial straight line, intermediate curved, and final straight line can be seen. However, in atomised copper powder preforms and in copper samples reduced at 1073K (800^{o}C) only

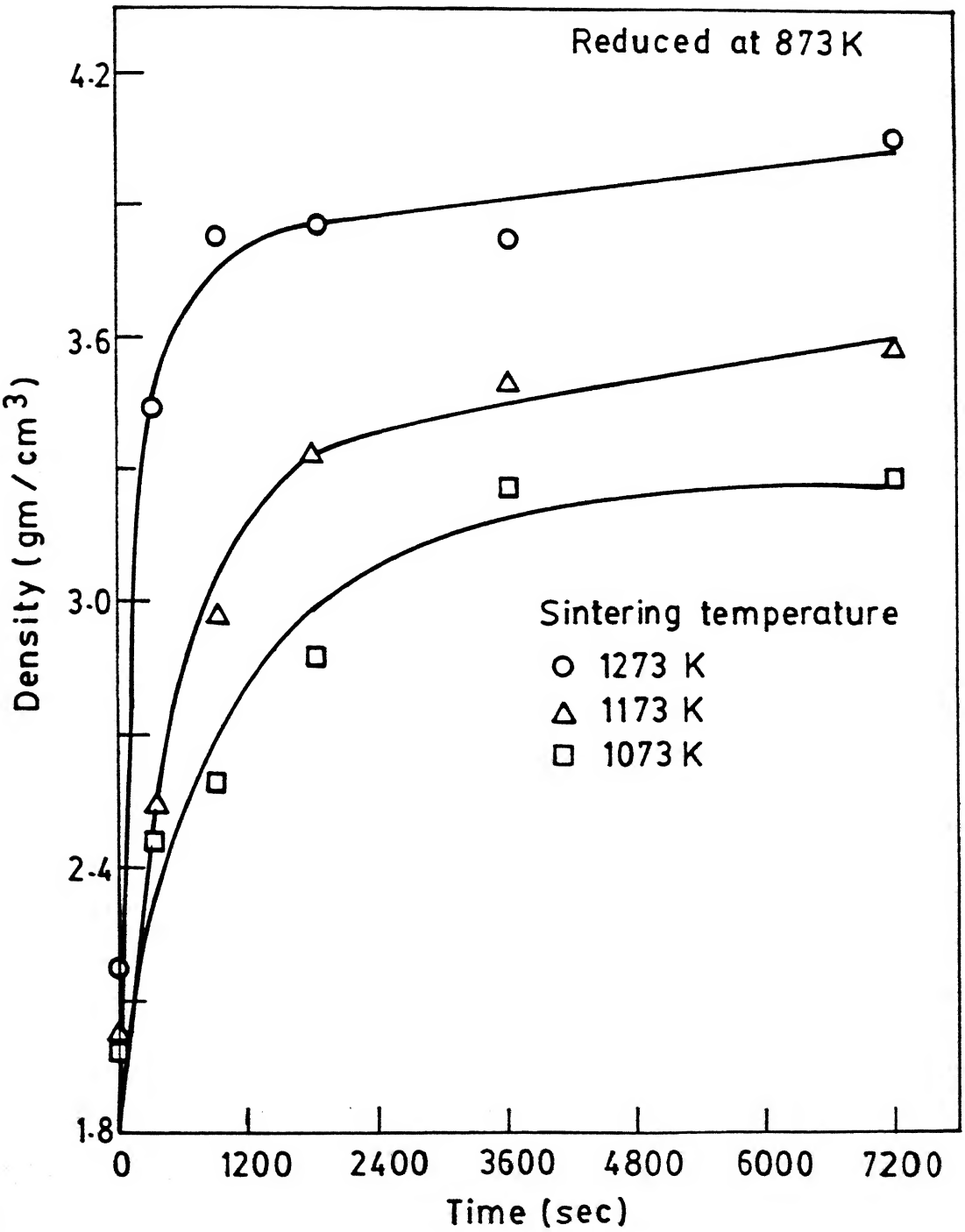

Fig. 4.5 Variation in Density of Copper Samples reduced at 873K for 5400 s as a function of sintering time and temperature.

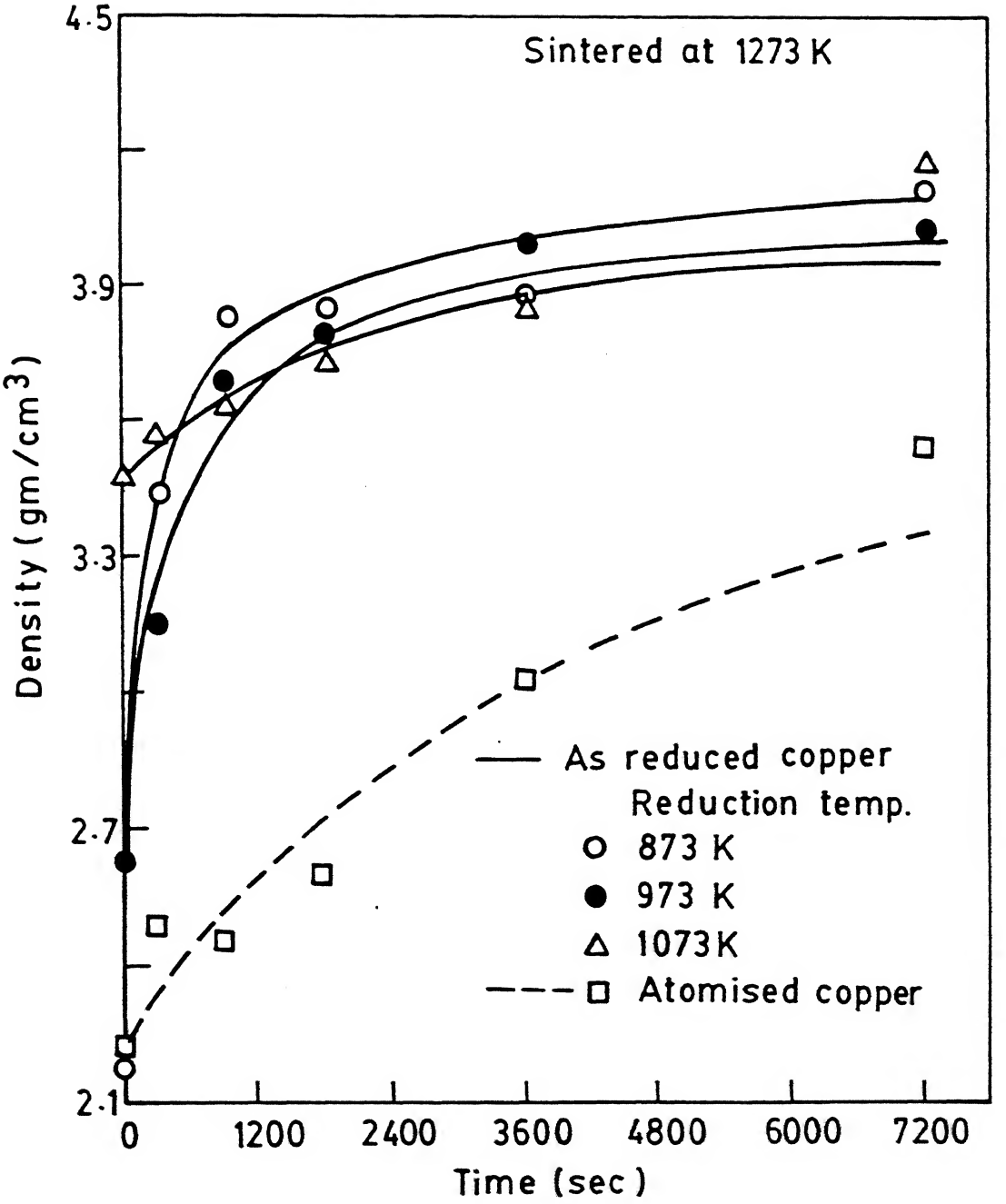

Fig. 4.6(a) Variation in sintered density as a function of sintered time and reduction temperature.

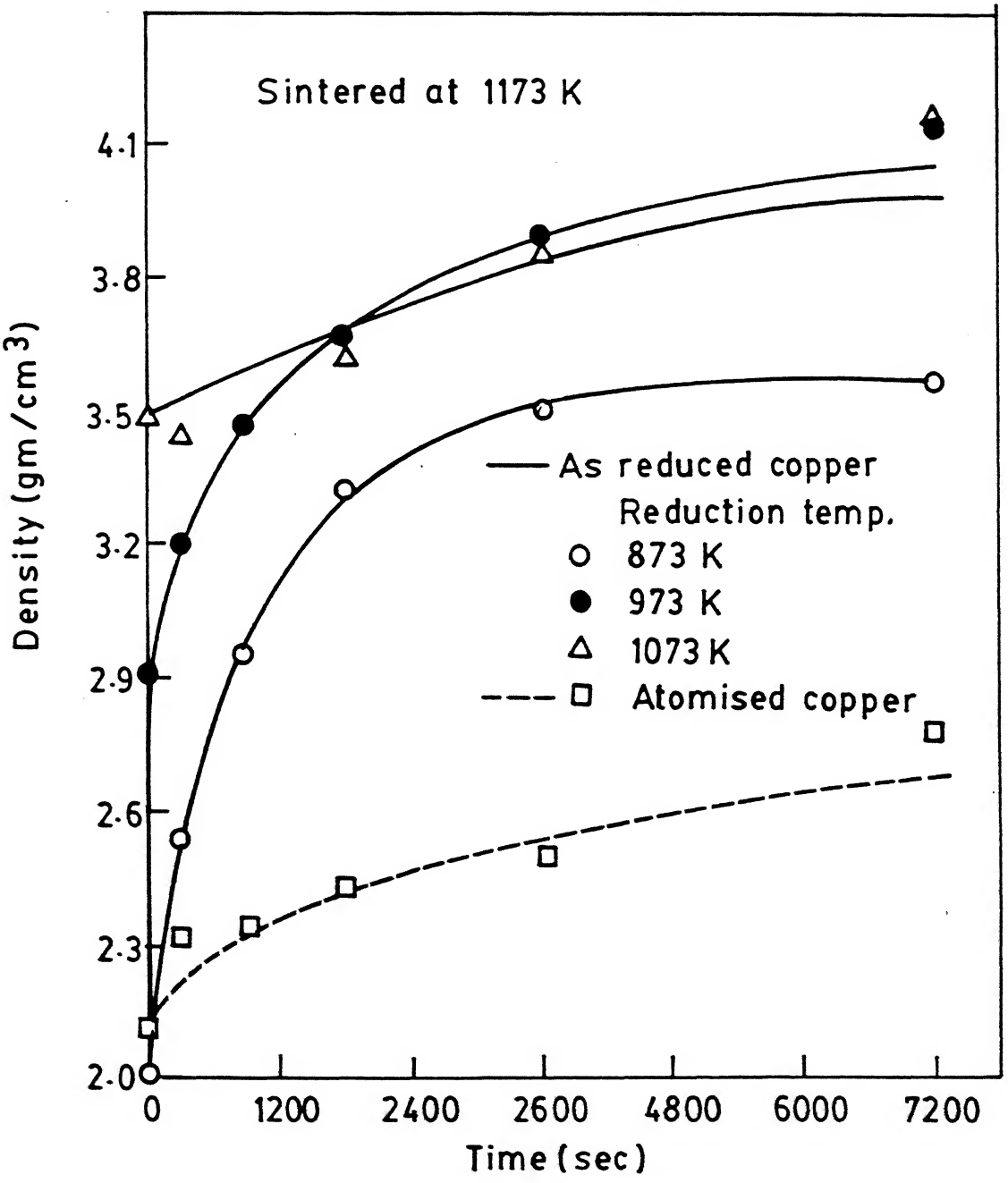

Fig. 4.6(b) Variation in sintered density as a function of sintering time and reduction temperature.

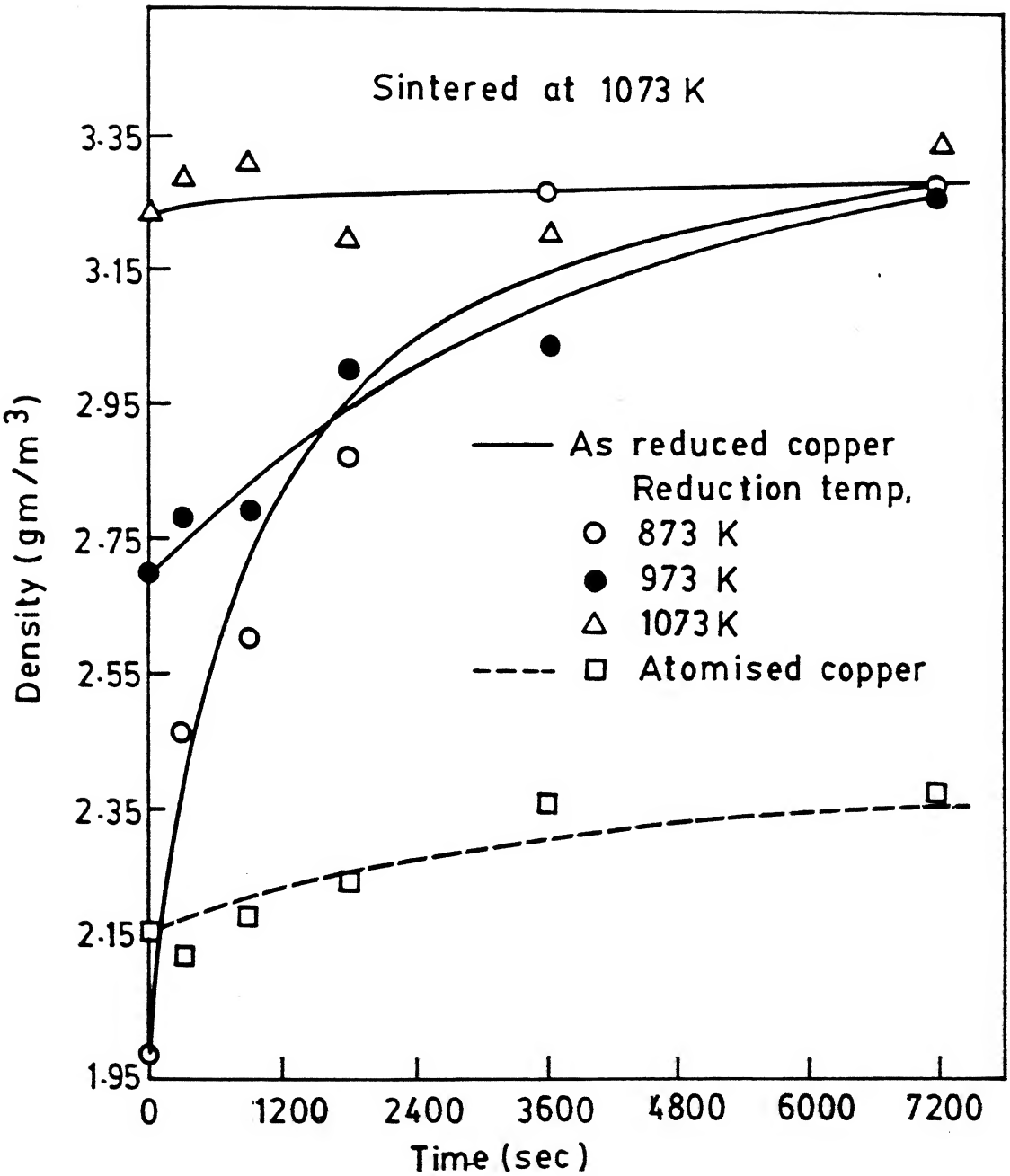

Fig. 4.6(c) Variation in sintered density as a function of sintering time and reduction temperature.

the last two regions are noticed when sintered at 1273K (1000°C) and 1173K (900°C). When the sintering temperature is 1073K (800°C) atomised copper preform and copper samples reduced at 1073K (800°C) show only the third region, thereby implying that as the sintering temperature approaches the temperature of reduction, the three- region curve moves towards the negative time axis and thus the curve begins at a later stage on the positive time scale. In general the rate of increase of density with respect to sintering time is higher in initial stages of sintering and then it decreases as signified by curved region and subsequently the rate of change in density drops to a very small value as can be seen in the third region showing flattening of the curve.

4.2.2 Variation of Rate of Change of Density($\partial \rho / \partial t$) as a Function of Sintered Density and Reduction Temperature:

The cuprous oxide preforms reduced at different temperatures for same period of time resulted in copper samples with differences in densities (Table 4.1) . The initial density for sintering of as-reduced samples were different. Therefore, rate of densification at a given density was obtained by obtaining a best fit equation for experimental data between sintered density and sintering time. The equation thus obtained was differentiated with respect to time and used for calculating the value for ($\partial \rho / \partial t$). This was plotted as a function of density. A lograthmic curve of type

$$\rho = A \ln t + B \quad \ldots (4.1)$$

where ρ is density, t is sintering time and A and B are constants, was found to be the best fit for samples reduced at 873K (600°C) and 973K (700°C) followed by sintering at 1273K (1000°C). For copper samples reduced at 1073K (800°C) followed by sintering at 1273K (1000°C) and those made from atomised copper powder and sintered at 1273K(1000°C), parabolic law of the type

$$\rho = C + D\sqrt{t} \quad \ldots (4.2)$$

where C and D are constants, was found to be the best fit. The values of constants are given in table 4.2.

Variation of rate of change of density($\partial\rho/\partial t$) as a function of sintered density and temperature of reduction when sintered at 1273K (1000°C) is shown in Figure 4.7. The same figure also shows the variation of $(\partial\rho/\partial t)$ with respect to density for the sintered compacts prepared from atomised copper powder. If can be seen that irrespective of the method of copper production, $(\partial\rho/\partial t)$ decreases as the density achieved in the copper compacts increases. The decrease in very sharp in the initial stages. Beyond a density of about 3.8 gm/Cm^3, the difference in $(\partial\rho/\partial t)$ values of various samples were not significant subsequently the value of $(\partial\rho/\partial t)$ approaches zero for all types of samples. Further, it can be seen that the value of $(\partial\rho/\partial t)$ at any given density for samples of atomised

TABLE 4.2

Value of Constants for the Variation of Density with Sintering time for Best Fit Equations for Samples Sintered at 1273K.

Copper Sample Type	Constants A	B	C	D
873 Reduced	0.1345	3.4084	-	-
973K Reduced	0.1296	3.3084	-	-
1073K Reduced	-	-	3.378	0.0737
Atomised Copper	-	-	2.0806	0.1269

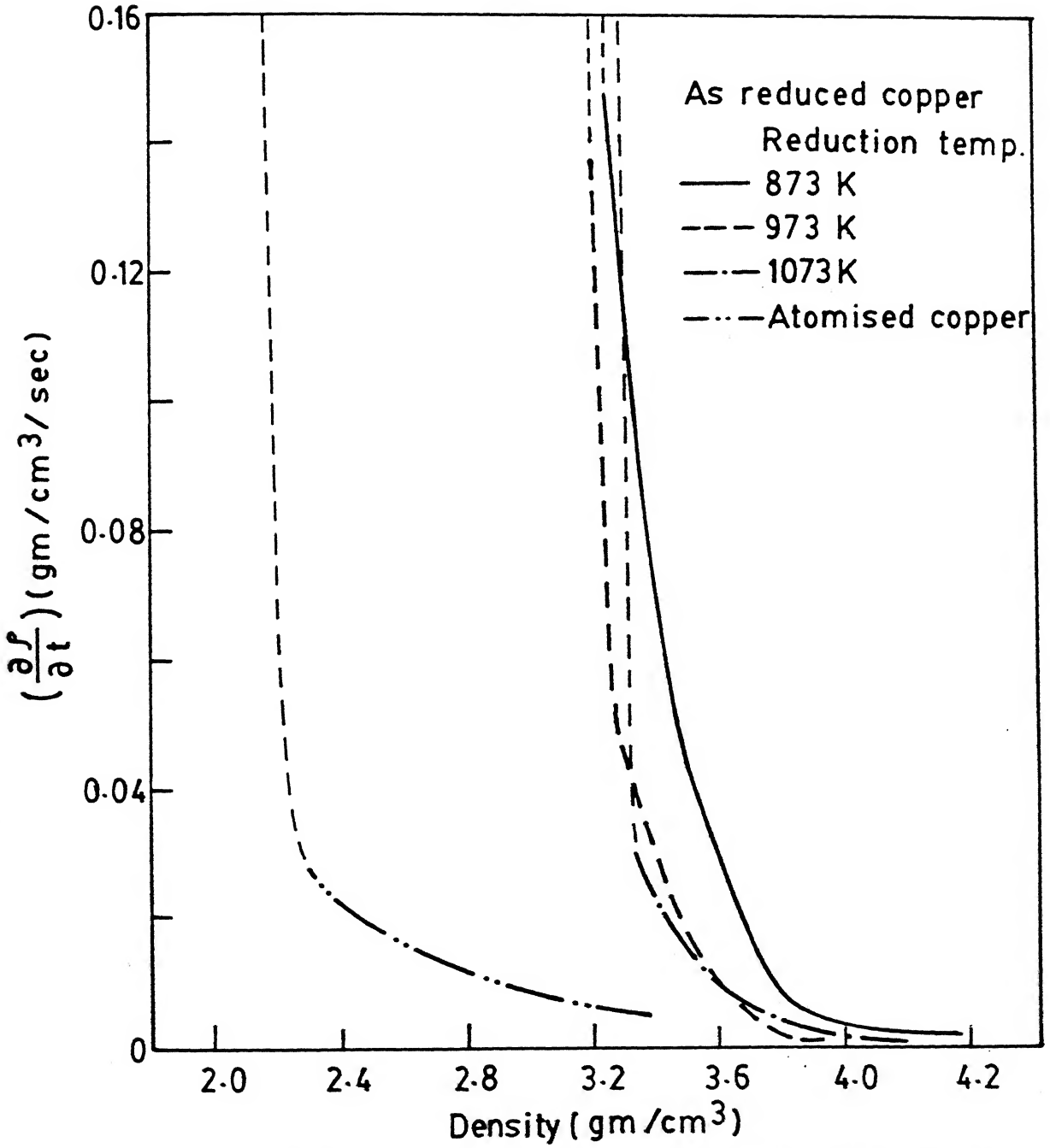

Fig. 4.7 Variation of rate of change of density as a function of sintered density and temperature of reduction when sintered at 1273K.

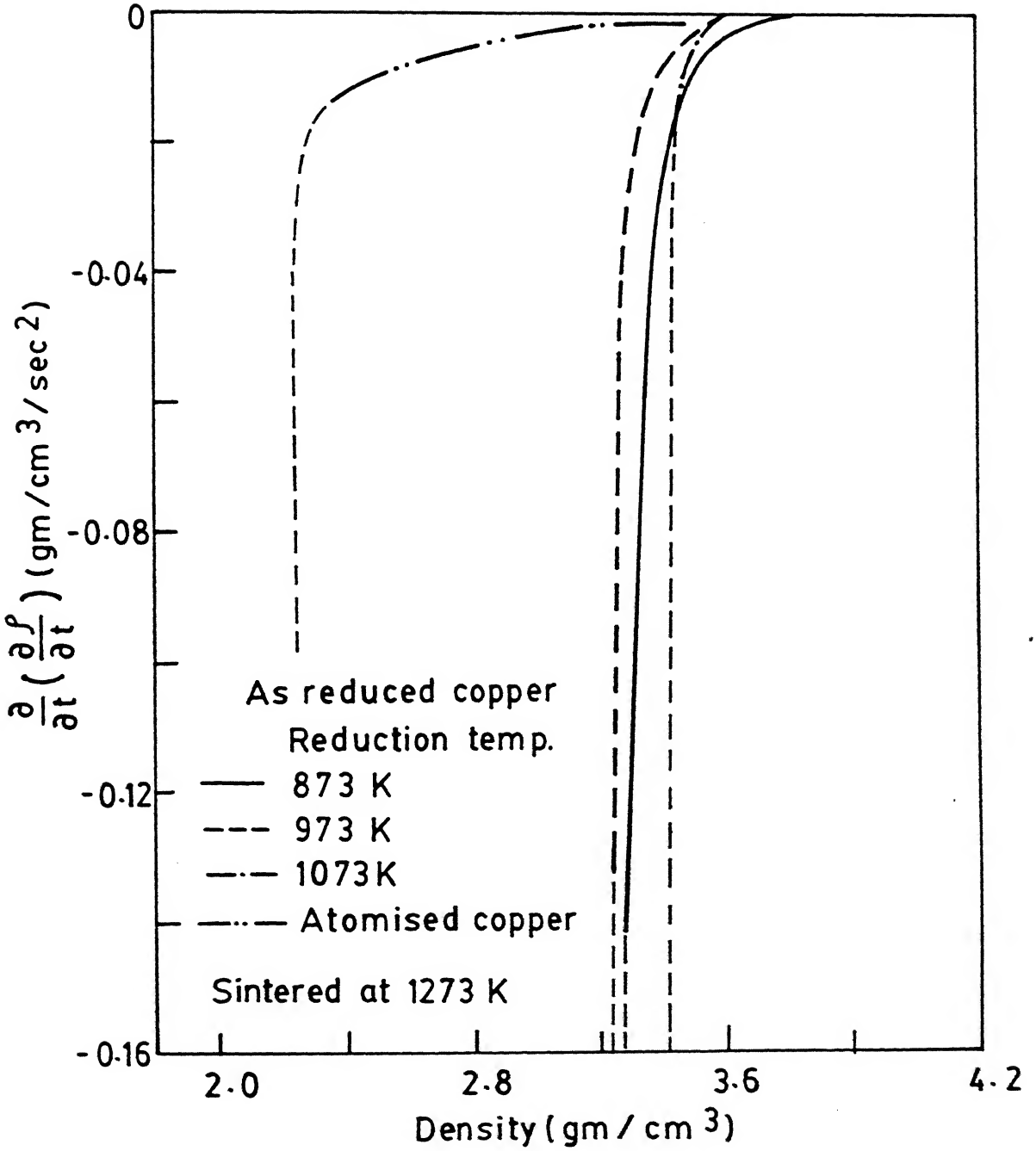

Fig. 4.8(a) Variation of $\frac{\partial}{\partial t}\left(\frac{\partial}{\partial t}\right)$ for copper samples reduced at different temperatures as a function of sintered density.

copper powder are much less than that in reduced copper samples. For example, at a density of about 3.4 gm/Cm^3 the values of$(\partial\rho/\partial t)$ for copper samples reduced at 873K (600°C), 973K (700°C) and 1073K (800°C) are 0.07, 0.04 and 0.03 gm/Cm^3-s whereas this value for atomised copper sample is only 0.006gm/Cm^3-s.

4.2.3 Variation of $\frac{\partial}{\partial t}(\frac{\partial}{\partial t})$ as a Function of Sintered Density and Sintering Time :

It is apparent from Fig. 4.7 that the rate of change of density decreases very fast initially, particularly for reduced copper samples indicating that the rate of densification is decreasing. The parameter $\frac{\partial}{\partial t}(\frac{\partial \rho}{\partial t})$ was calculated by further differentiating the $(\frac{\partial \rho}{\partial t})$ equations withrespect to time. This parameter is of interest because it reveals the rate at which the rate of change in density decreases. This parameter was plotted as a function of both sintered density and sintering time.

The variation of $\frac{\partial}{\partial t}(\frac{\partial \rho}{\partial t})$ as a function of sintered density for copper samples reduced at different temperature and followed by sintering at 1273K (1000°C) is shown in Fig. 4.8(a). Fig. 4.8(b) shows the variation of $\frac{\partial}{\partial t}(\frac{\partial \rho}{\partial t})$ as a function of sintering time for copper samples reduced at different temperatures and followed by sintering at 1273K. The nature of curve obtained in Fig. 4.8(a) is similar to that observed in Fig. 4.7, viz variation of $(\frac{\partial \rho}{\partial t})$ with respect to sintered density.

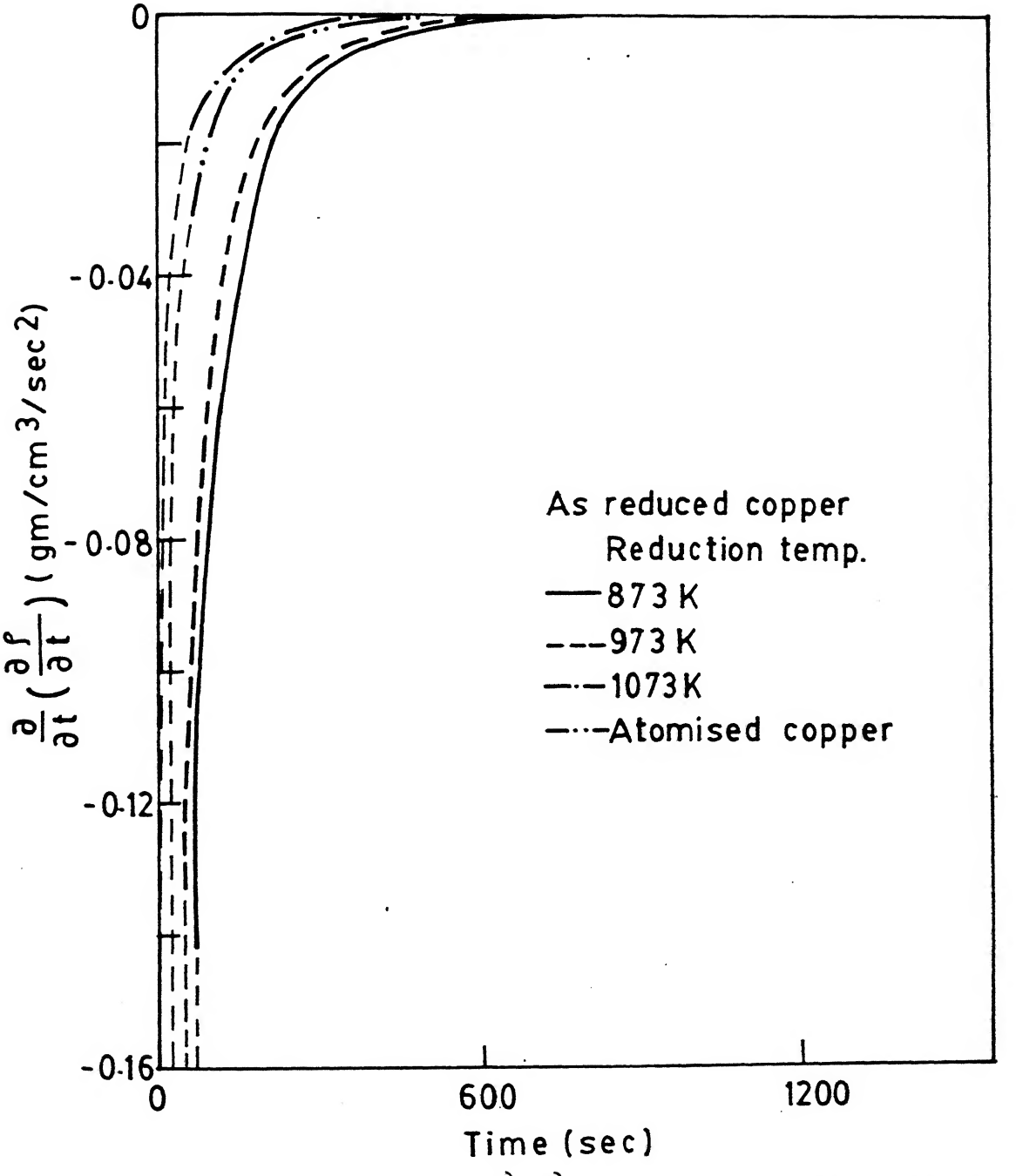

Fig. 4.8 Variation $\frac{\partial}{\partial t}(\frac{\partial}{\partial t})$ as a function dintered density for copper samples reduced at different temperatures.

However, it can be seen that this parameter when plotted as a function of sintering time (Fig. 4.8(b)) indicates that for any given time the rate of increase in ($\frac{\partial \rho}{\partial t}$) is more negative in samples reduced at 873K (600°C) and least negative in samples reduced at 1073K (800°C). After around 600 s (10 min.) of sintering the rate of change in ($\frac{\partial \rho}{\partial t}$) i.e. the value of $\frac{\partial}{\partial t}$ ($\frac{\partial \rho}{\partial t}$) becomes almost zero for all the samples.

4.2.4 Variation of Relative Shrinkage per Unit Mass as a Function of Sintering Time and Temperature of Reduction:

The density represents simply the mass contained in a unit volume. The densification of powder materials, when subjected to temperature, occurs by the shrinkage of a reference volume surrounding a fixed number of particles. Therefore if one wishes to monitor the progress of sintering in terms of the reduction of free surface area per particle, density or relating density cannot be regarded as the true consolidation parameter. A true consolidation parameter must be defined on the basis of per unit mass rather than per unit volume. The usage of relative shinkage per unit mass H has been suggested by Bhargava (15). Thus

$$H = \frac{\rho - \rho_o}{\rho(1-\rho_o)} \qquad \ldots(4.3)$$

where ρ_o and ρ are the relative densities before and after sintering. From the definition of H, it can be seen that

its value, for any value of initial relative density, ρ_o, will be zero at the start of sintering and will attain a value of one at the end of the densification. Thus its usage also eliminates the effect of initial relative densities which were different for samples produced by reducing Cu_2O preforms at different temperatures. Equation 4.3 was used to calculate the relative shrinkage per unit mass at various levels of densification of samples and was plotted as a function of sintering time and temperature of reduction to study its nature.

Variation of relative shrinkage per unit mass as function of sintering time and temperature of reduction for as-reduced samples is shown in figure 4.9(a), 4.9(b) and 4.9(c) for sintering temperatures of 1273K (1000°C), 1173K (900°C) and 1073K (800°C) respectively. The maximum relative shrinkage per unit mass is observed in samples reduced at 873K (600°C) and minimum in those reduced at 1073K (800°C). After 5400s (90 min.) of sintering time the relative shrinkage becomes stable and not much shrinkage occurs thereafter.

4.2.5 Variation of Total Contact Area per Particle as a Function of Sintering Time and Reduction Temperature:

Concepts of relative porosity and relative shrinkage per unit mass is utilized by viewing the powder aggregate as a tesselation created in space. By describing a powder preform in terms of Dirichlet tesselation, Bhargava (15) has concluded that a relationship between

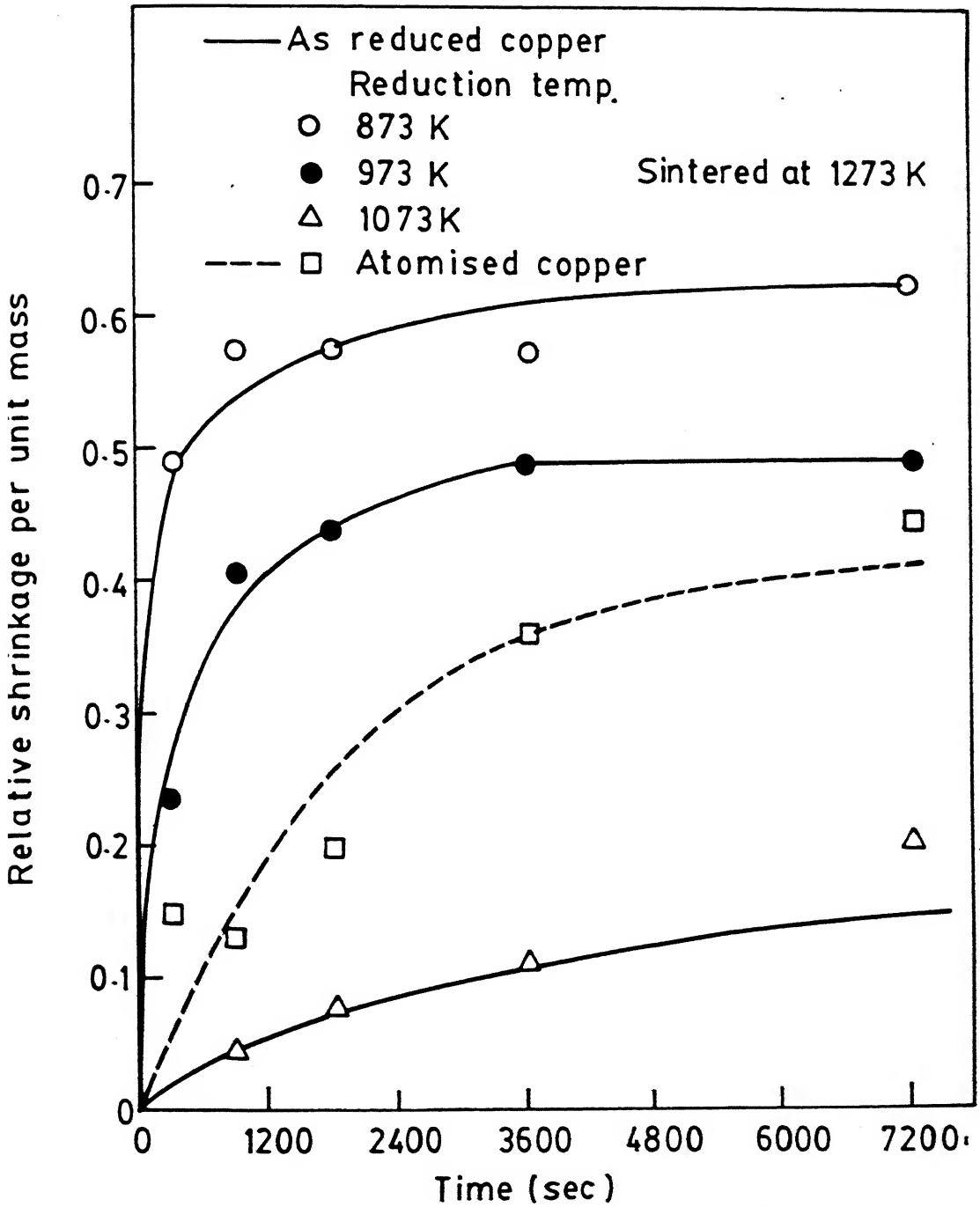

Fig. 4.9(a) Variation of relative shrinkage per unit mass as a function sintering time for as-reduced copper samples sintered at 1273K.

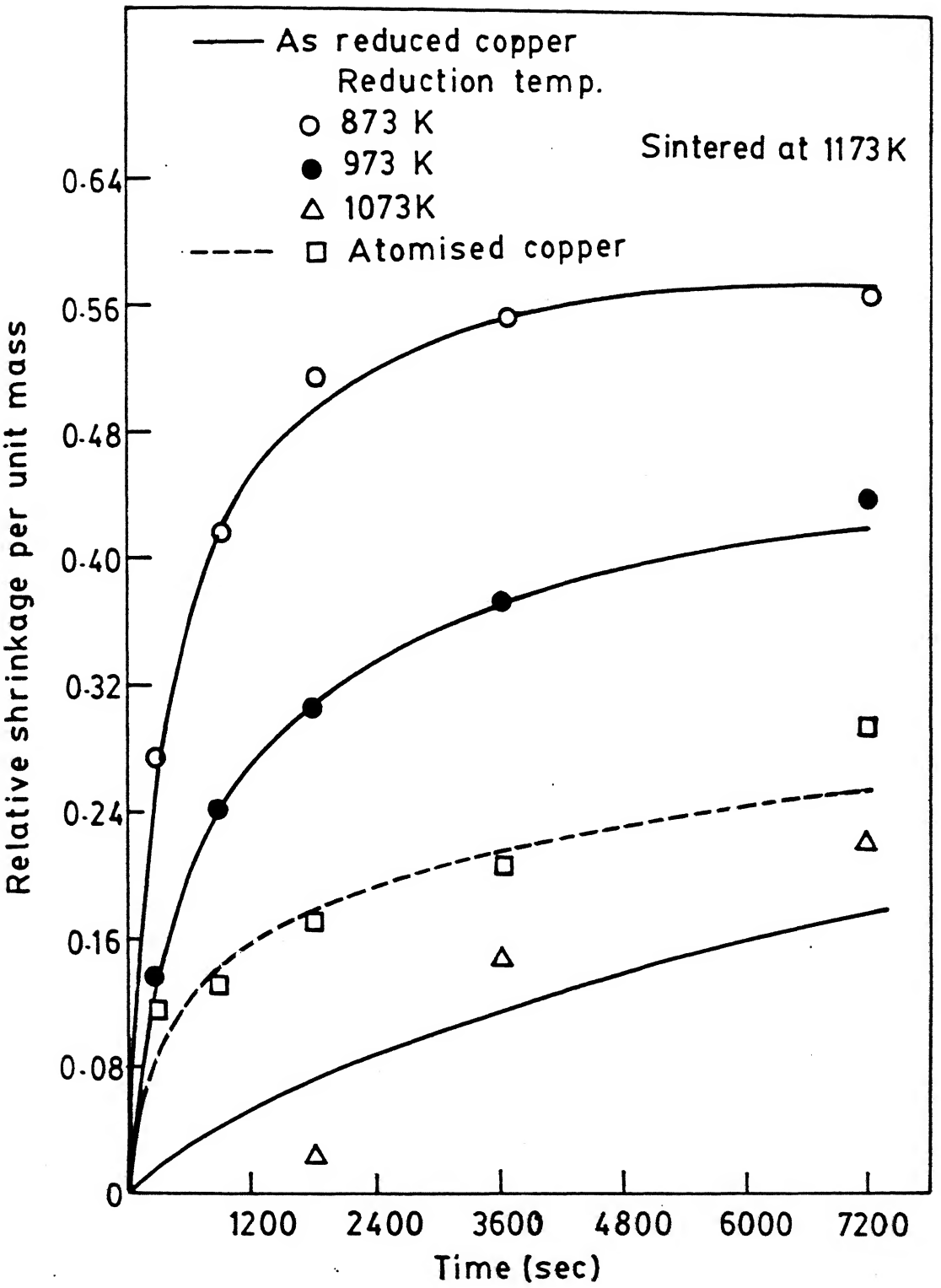

Fig. 4.9(b) Variation of relative shrinkage per unit mass as a function sintering time for as-reduced copper samples sintered at 1173K.

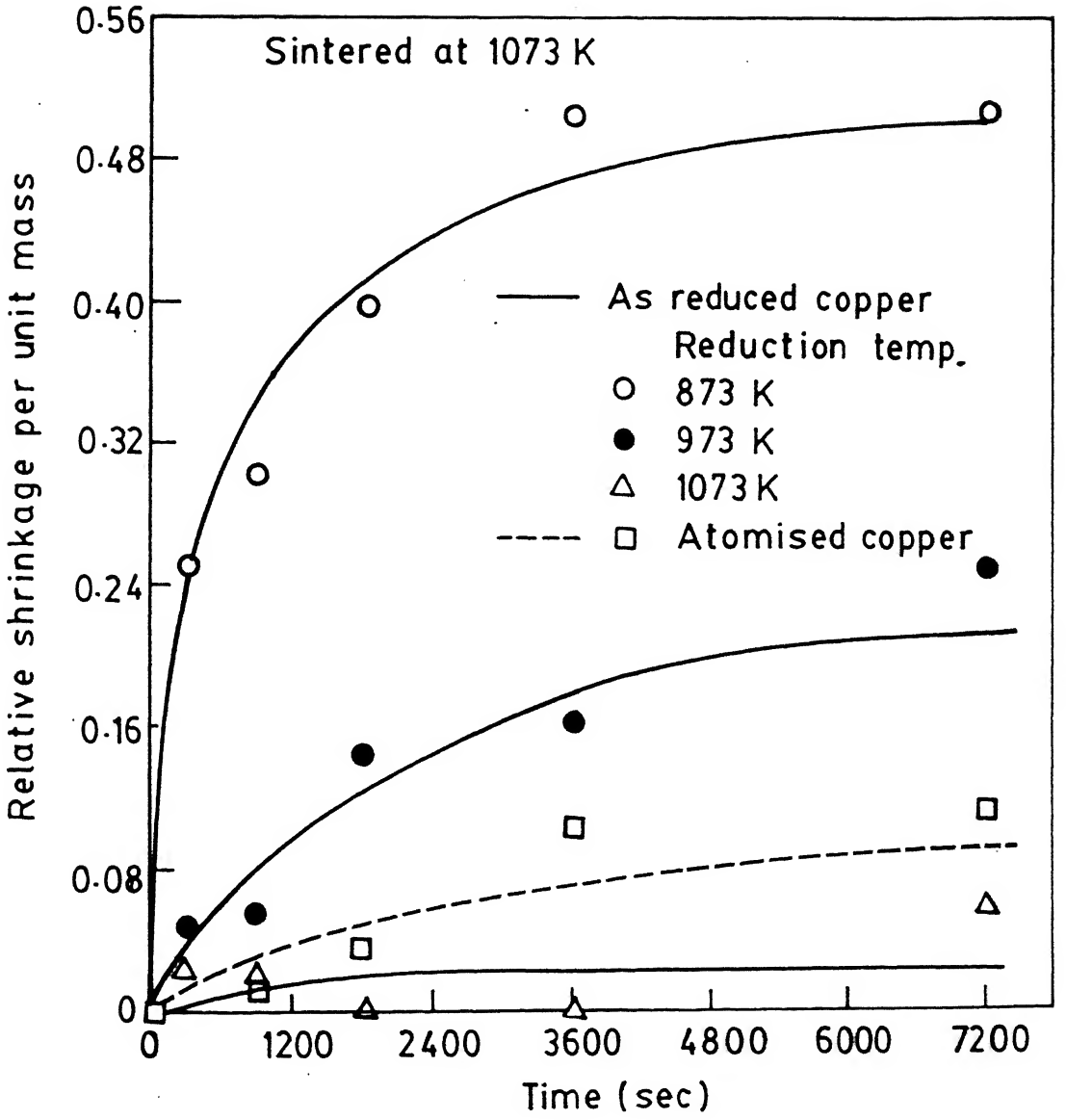

Fig. 4.9(c) Variation of relative shrinkage per unit mass as a function of sintering time for as -reduced copper samples sintered at 1073K.

total relative free surface area per particle and the relative shrinkage per unit mass, exists. The relationship is

$$\frac{S_F}{S_o} = [\ 1-H\ ]^{2/3} \qquad \ldots (4.4)$$

where,

S_F = Total free surface area after consolidation

S_o = Total free surface area before consolidation

H = Relative shrinkage per unit mass of powder aggregate.

and

$$\frac{S_C}{S_F} = \frac{1-[1-H]^{2/3}}{[1-H]^{2/3}} \qquad \ldots (4.5)$$

Where S_C is total contact area.

The equation 4.5 was utilized to calculate the total contact area per particle at a given density.

Figure 4.10 shows the variation of total contact area per particle as a function of sintering time and reduction temperature when sintered at 1273K (1000°C) It can be seen that the increase in total contact area per particle is maximum in samples reduced at 873K (600°C) and minimum in samples reduced at 1073 (800°C). These curves were plotted using best fit equations obtained on an IBM PC XT with the help of GRAPHER package. The best fit

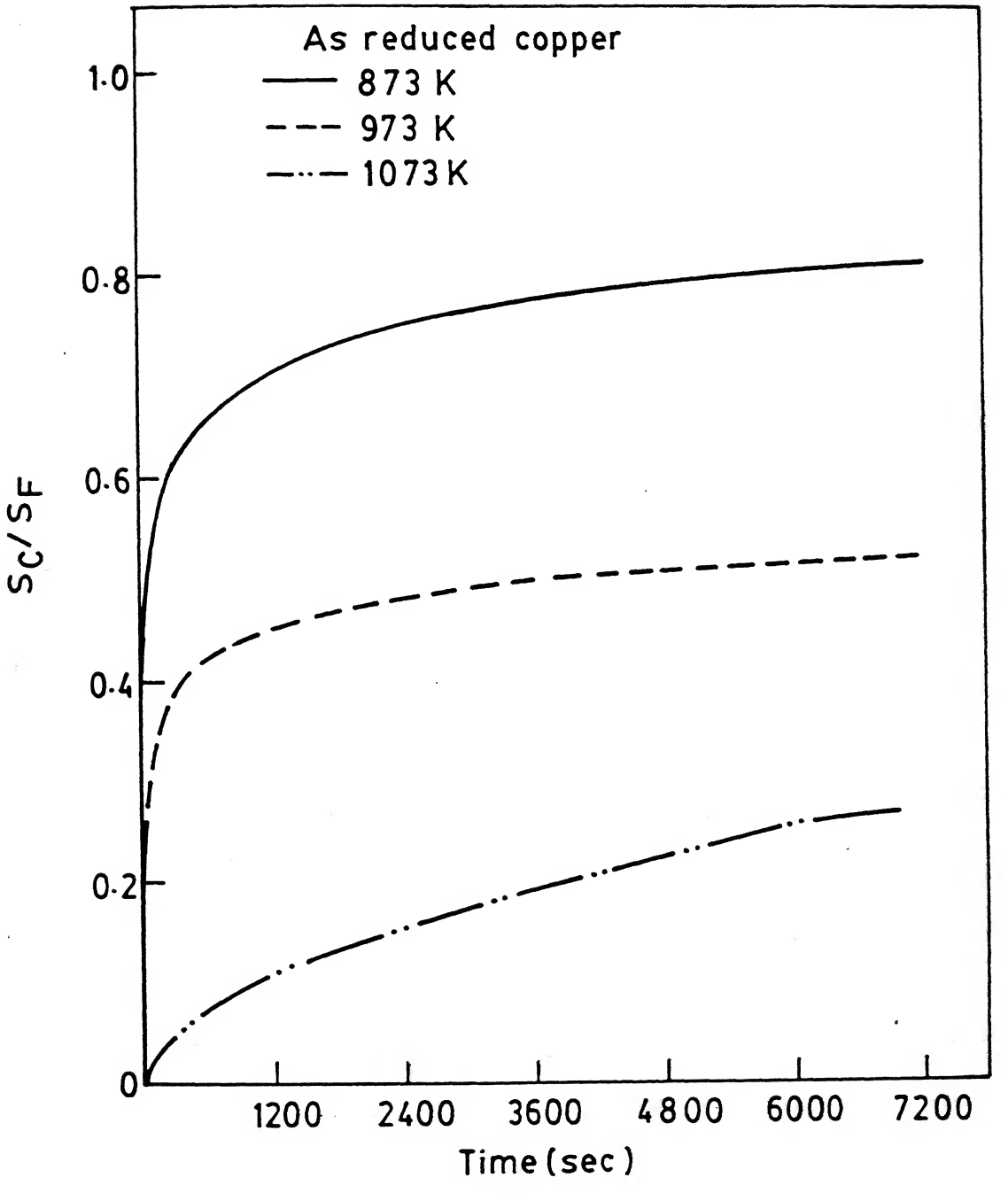

Fig. 4.10 Variation of total contact area per particle as a function of sintering time and reduction temperature for samples sintered at 1273K.

equation for total contact area per particle as a function of time was obtained by using the values of total contact area per particle calculated from experimental data. For copper samples reduced at 973K (700°C) and 873K (600°C) followed by sintering at 1273K (1000°C), a logarithmic curve of the type

$$\frac{S_C}{S_F} = A \ln t + B \qquad \ldots (4.6)$$

where A and B are constants and t is sintering time, was found to be the best fit. Whereas for samples reduced at 1073K (800°C) and for samples of atomised copper powder when sintered at 1273K (1000°C) a power law of the type

$$\frac{S_C}{S_F} = C(t)^D \qquad \ldots (4.7)$$

where C and D are constants was the best fit. The values of constants are given in Table 4.3.

4.2.6 Microstructural Studies of Sintered Samples:

Sintering involves changes in both inter-particle and intra-particle pore morphology of powder compacts. Therefore, in order to have better understanding of these changes microstructural studies by optical and as well as seanning electron microscope were carried out. The samples reduced at 873K (600°C) and 1073K (800°C) followed by sintering at 1273K (1000°C) were chosen to study this aspect. They represented the two extreme conditions as far as the pore morphology and the defects introduced in the copper powder during

TABLE 4.3

Value of Constants for the Variation of S_C/S_F with Sintering time for Best Fit Equations.

Copper Sample Type	Constants			
	A	B	C	D
873K Reduced	0.063	0.52166	-	-
973K Reduced	0.041	0.3281	-	-
1073K Reduced	-	-	0.0194	0.5609
Atomised Copper	-	-	0.0291	0.609

reduction of oxide is concerned.

The SEM micrographs of fractured surface of samples reduced at 873K (600°C) and sintered at 1273K (1000°C) for 3600 s (60 min.) is shown in Figure 4.11. As discussed earlier the various nucleated and grown Cu islands sinter together as sintering progresses. On comparing Figure 4.1(b) with Figure 4.11(a) and 4.11(b) it can be seen that in the case of 873K (600°C) reduced copper sample the neighbouring nucleated and grown copper islends have sintered together to form a bigger cconglomerate. However fine porosity between the neighbouring islands still persists . In contrast Figure 4.12(a) and 4.12(b) show the SEM micrograph of copper sample reduced at 800°C and sintered at 1000°C for 7200 s. It can be seen from these micrographs that the sintering between different island have occured, but no fine porosity, as shown in Figure 4.11 (a) and 4.11(b) exists in the sample.

4.3 Sintering Behaviour of Reduced and Compacted Copper Samples:

The densities of copper compacts obtained by hydrogen reduction of cuprous oxide preforms for 5400 s (90 min.) at various temperatures was found to be different (Table 4.1).As discussed earlier, different densities mean that the particle arrangement and extent of sintering in the samples was different . In view of the sintering

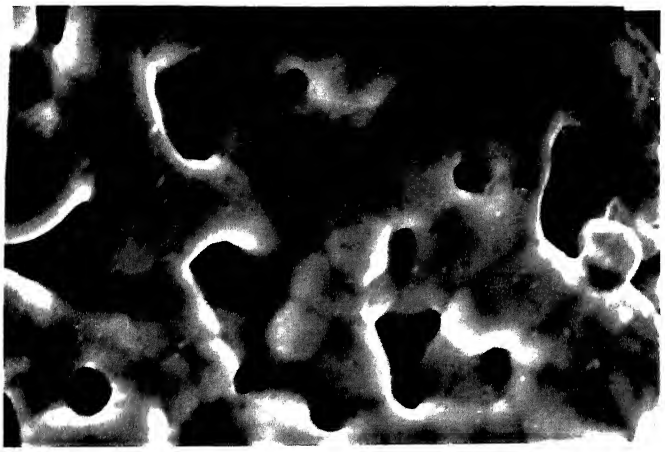

(a)

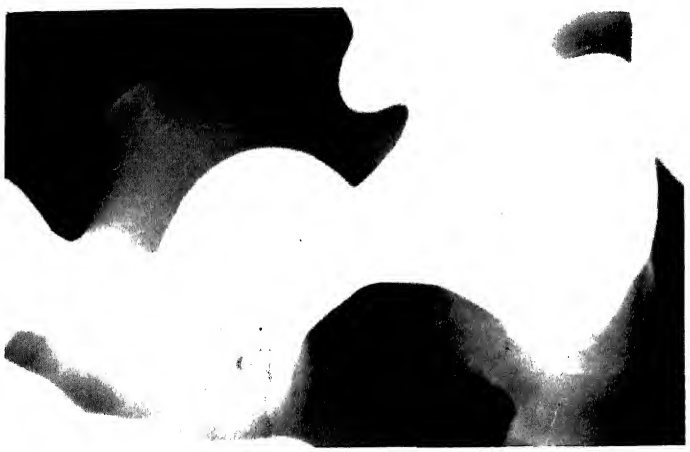

(b)

Fig. 4.12 SEM micrograph of copper samples reduced at 1073K and sintered at 1273K for 7200 s (a) 3500X (b) 3700 X.

behaviour of any powder material being closely related with the arrangement of particles in the sample it was expected that difference in initial densities may have affected the sintering behaviour of the as-reduced copper samples.

In order to investigate the above fact the reduced copper samples and compacts prepared from atomised copper were roll- compacted to get similar initial densities. The samples reduced at 873K (600°C) and 1073K (800°C) were only used for studying the effect of initial density on its sintering behaviour. Cold rolling of sintered porous metal compacts/strips have been reported by several workers (14). It has been found that, depending upon the initial density of sintered porous metal compacts/ strips, in the initial stages of cold rolling the particles undergo rearrangement and restacking and very little cold working of powder particles takes place. As the cold rolling progresses, a stage comes when powder particles undergo plastic deformation. In the case of sintered porous copper compacts/ strips, in the initial stages of cold rolling the particles undergo rearrangement and restacking and very little cold working of powder particles takes place. As the cold rolling progresses, a stage comes when powder particles undergo plastic deformation. In the case of sintered porous copper compacts/ strips it has been shown that rearrangement and restacking of powder particles take place till about 40-45% cold rolling for the compacts/strips of initial relative density

of about 0.4 . The maximum limit of cold rolling thickness reduction without causing plastic deformation of particles would increase as the initial density of strip/ compact decreases. In the present case, the relative densities of as -reduced copper samples are in the range of 0.22 to 0.44, as shown in Table 4.1.

As discussed in 3.5, the maximum cold rolling given to as-reduced copper sample was 43%, it can be infirred that negligible plastic deformation of particles occured in the cold rolled copper compacts.

Table 4.4 shows the density of various reduced copper compacts after cold rolling. It can be seen that the samples had densities within 2.7-3.25 gm/Cm^3. Fig. 4.13 shows the variation of sintered density as a function of sintering time for copper compacts obtained after reduction at different temperatures. It can be observed that even though the initial densities were similar, the density of samples reduced at 873K (600°C) have a much higher value when sintered at 1273K (1000°C) for 7200 s (120 min.) than those obtained in samples reduced at 1073K (800°C) and compacts prepared from atomised copper powder sintered under similar conditions.

Fig. 4.14 (b) shows the variation of relative shrinkage per unit mass as a function of sintering time for compacts obtained by reducing cuprous oxide compacts at different temperatures followed by sintering at 1273K (1000°C). It can be seen that compacts reduced at 873K (600°C) show maximum relative shrinkage per unit mass

TABLE 4.4

Density and Relative Density of Reduced Copper Compacts After Cold Rolling .

Copper Sample Reduced at	Density gm/Cm^3	Relative Density
873K	2.68	0.3
1073K	3.25	0.36

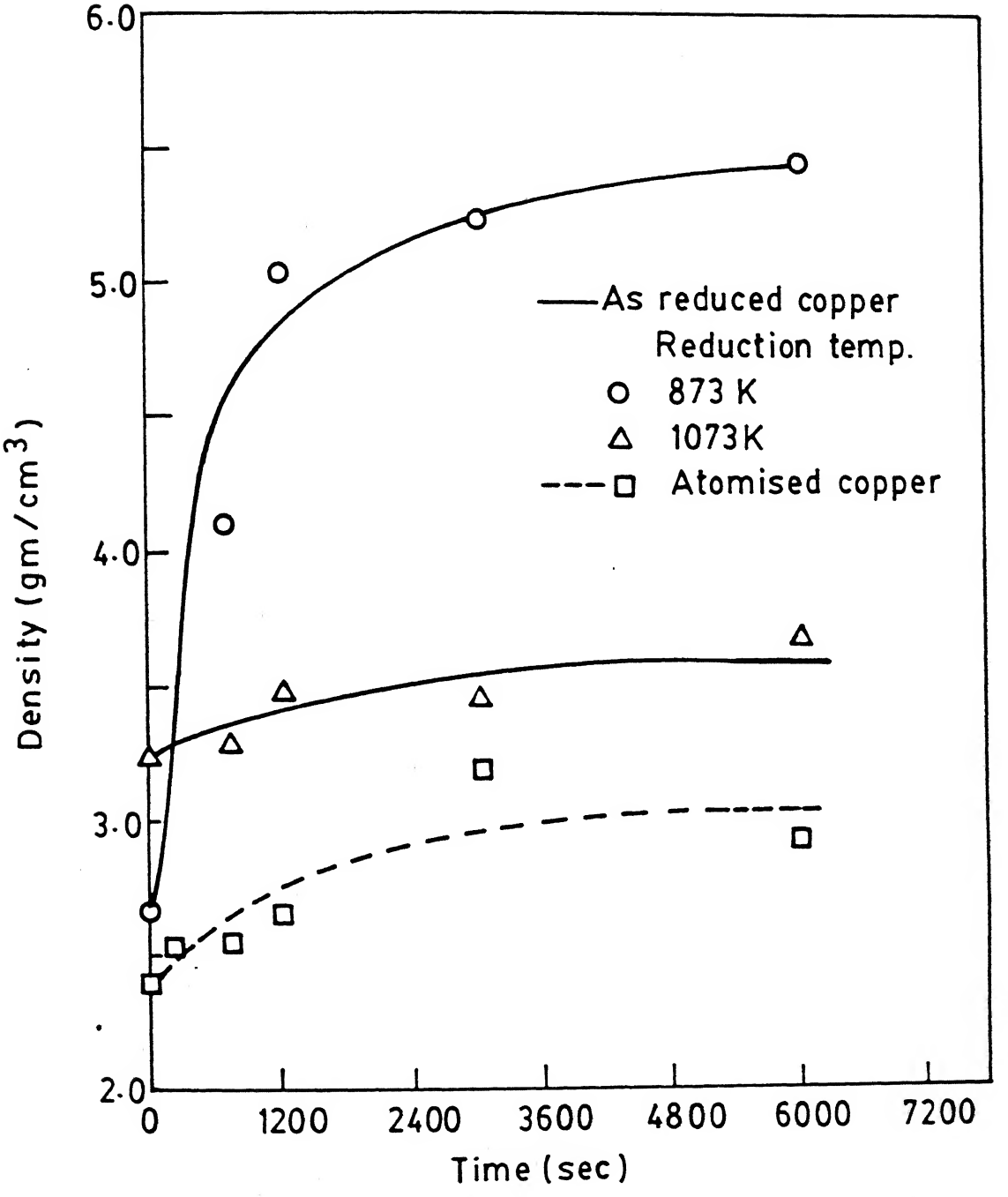

Fig. 4.13 Variation of sintered density as a function of sintering time for cold rolled reduced copper compacts sintered at 1273K.

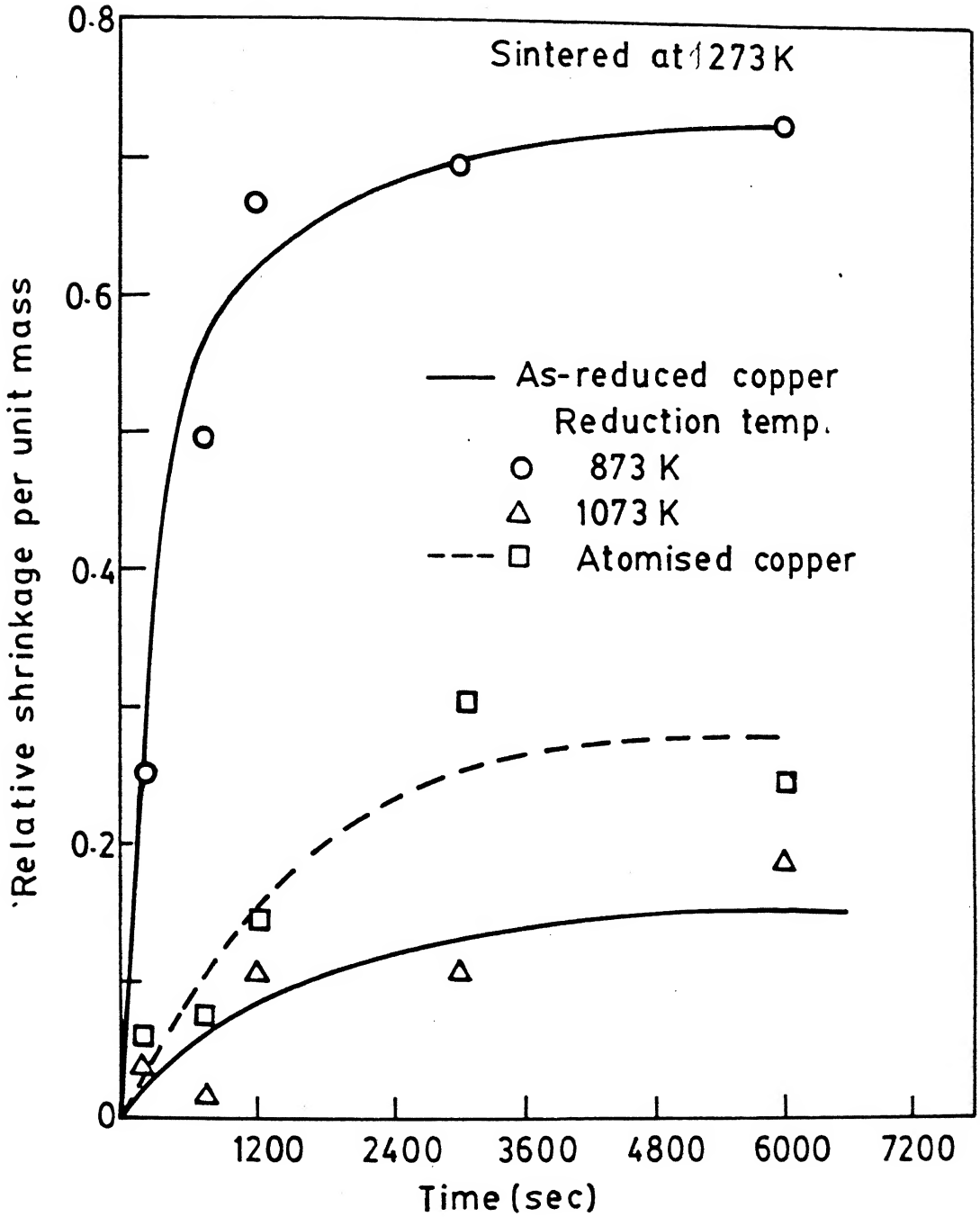

Fig. 4.14 Variation of relative shrinkage per unit mass as a function of sintering time for cold rolled copper compacts sintered at 1273K.

relative shrinkage per unit mass when sintered at 1273K (1000°C) . Compacts of atomised copper powder show higher relative shrinkage per unit mass than compacts reduced at 1073K (800°C) under similar sintering condition. The sintering behaviour in reduced and then compacted samples is similar to those observed in as-reduced ssamples under similar condition of sintering (Fig. 4.9(a) - (c)).

CHAPTER -V

DISCUSSION

As shown in the previous chapter the sintering behaviour of copper samples produced by reducing cuprous oxide preforms at different temperatures, differed considerably. Such a difference is related to different morphologies of copper formed by the solid state reduction of cuprous oxide. Results on the sintering behaviour of copper samples can therfore be understood in terms of morphological differences, their origin and evolution , during the course of hydrogen reduction of cuprous oxide.

5.1 Wagner's Mechanism of Cuprous Oxide Reduction:

Cuprous oxide like wustite, cobalt and nickel oxides is a metal deficit, i.e. a p-type semiconductor with the formula $Cu_{2-x}\ O$ (16) with $x<10^{-3}$; x depends primarily on temperature and oxygen partial pressure at the time of of its forming. When cuprous oxide lattice is brought in contact with the reducing gas such as hydrogen the chemical reaction takes place at the surface.

The reduction reaction of cuprous oxide by hydrogen can be understood in terms of Wagner's theory of non-stoichiometric oxide reduction. The chemical reaction at the surface is as follows:

$$(H_2) + O^{-2} + 2Cu^{+} \square \longrightarrow (H_2O) + 2Cu \quad \ldots (5.1)$$

involving the transfer of one oxygen ion from the oxygen lattice to the gas, the conversion of two cuprous ions to copper, and the migration of the associated vacancy ($\square$) from the copper lattice to the surface where it vanishes. As a result of the phase boundary reaction, the Cu/O ratio of the oxide at the surface increases above the saturation level and causes supersaturation. Thus, the activity of copper at the surface increases as the reaction proceeds and eventually exceeds that of metallic copper (unity).. When the surface activity of copper reaches a critical value, which is high enough locally for nucleation, copper nucleus is formed, preferably at some defect on the surface.

Under suitable conditions of reduction, nucleation of copper phase takes place after the oxide surface becomes supersaturated. The diffusivity of copper ions in the oxide lattice is high at 873K (600^{o}C) and 1073K (800^{o}C) and it is likely that the capacity of copper ions generation is of the same order of magnitude as their capacity of transport from the surface inwards and there exists a situation of mixed type of control.

Under conditions of mixed type of control niclei grow from two sources-diffusion of copper ions from the bulk, and that generated freshly at the surface making them into the shape of semi-spherical or spherical

islands (Figure 4.2). During the subsequent stage of reduction, the copper nucleated and grew at more points and slowly covered the entire surface. After the entire surface had been covered with the first layer of reduced copper, further penetration of hydrogen to the copper/cuprous oxide interface occurs by diffusion through the newly formed pore channels between the different copper islands. When hydrogen becomes available to the next reaction interface, further nucleation of copper occurs there. Nucleation and growth of copper in the second layer, as a result of the chemical reaction occuring at the reaction interface, were accompanied by the formation of gaseous H_2O. Gaseous H_2O first diffuses outward through the newly formed pore channels and then to the bulk stream through the pores existing in the initial preform.

5.2 Exothermic Heat of Chemical Reaction and Intra-Particle and Inter-Particle Sintering:

Reduction reaction of cuprous oxide with hydrogen is highly exothermic. Once the entire surface is covered with freshly nucleated copper, subsequent reaction occurs by hydrogen penetration to the interface. The reduction below copper nuclei is also accompanied by H_2O gas and exothermic heat. Dissipation of heat by conduction through the first layer of copper is expected to raise the temperature which promotes sintering between spherical or hemispherical islands of copper. As the number of layers

of reduced copper increased, the outermost shell of copper was subjected to continuous heating as result of the dissipation through it of the exothermic heat and furnace heat. and thus became the most sintered layer. Therefore, the amount of intra-island porosity increased in the particle in a readily inward direction. Some sintering also occured between a number of the particles of reduced copper.

5. 3 Effect of Reduction Temperature on Internal Structures:

As pointed out by Wagner, the reduction of nonstoichiometric oxides such as Cu_2O involve the migration of vacancy from the copper lattice to the surface. Lower the temperature of reduction lower is the mobility of vacancies and copper atoms. Therefore, the defect concentration is more at lower temperatures of reduction than at higher temperatures. The X- ray analysis carried out to measure the internal strain and particle size of copper formed after oxide reduction failed to yield results because, the particle size after reduction was more than 2 μm. The X-ray analysis for the measurement of strains in samples with particle size greater than or close to 2 μm is not recommended. The highly exothermic nature of reaction, which results in excessive inter-nuclei and inter-particle sintering is the main reason for getting large particle size. However, Salewski (13) working with

tungsten oxide (WO_3 and $W_{20}O_{58}$) was able to show that internal strain (a measure of internal defect concentration) decreases whereas the particle size increases with increasing temperature of reduction. Salewski carried the tungsten oxide reduction in the temperature range of 0.25 Tm to 0.3 Tm with reaction not being highly exothermic, whereas the temperature range in which cuprous oxide reduction was carried out was in the range of 0.35 Tm to 0.75 Tm with reaction being highly exothermic. Thus one can account for the large particle size obtained after cuprous oxide reduction. However, since the formation of both Tungsten and copper by reduction of their oxides occurs by nucleation and growth.It can be concluded that as in the case of W internal strain i.e. internal defect concentration decreases with increase in reduction temperature in copper also.

5.4 Sintering Kinetics of Copper Compacts Obtained after Reducing Cu_2O Preforms at Different Temperatures:

Sintering behaviour is known to be affected by surface area both internal as well as external. The presence of intra-particle porosity has the effect of dividing the particle into much smaller sub-units i.e. islands / conglomerate of islands. This therefore decreases the distance through which defects will have to move to get annihilited. The pore structure gets rounded resulting in densification. Densification occuring

in copper samples produced by reduction at different temperature therefore can be explained in terms of sintering occuring within the conglomerates of islands and sintering between different conglomerates of islands.

Initially observed high sintering rate in copper sample produced by reduction of Cu_2O at 873K and 973K is because of high super saturation of defects in copper phase formed at these temperatures. This is in conformity with microstructure (Fig. 4.3 and Fig. 4.4) indicating the absence of annealing twins in samples reduced at 873K as against that in 1073K in which the defects have annihilated because of higher reduction temperature and higher exothermic heat. The absence of defects in samples produced by reduction at 1073K region one of the sintering curve is not observed. It is interesting to note that microstructure of 873K reduced and 1273K sintered for 7200 s, corresponding to a density of about 4 gm/cc. shows annealing twins (Fig. 4.15) indicating the annhilation defects occuring during sintering. Since the defect concentration after sintering for 5400 s became similar, the sintering kinetics in all the compacts also becomes similar as indicated by ρ vs t , $\frac{\partial \rho}{\partial t}$ vs ρ, $\frac{\partial}{\partial t}(\frac{\partial \rho}{\partial t})$ vs ρ and $\frac{\partial}{\partial t}$ $(\frac{\partial \rho}{\partial t})$ vs t plots shown in Fig. 4.6, 4.7 and 4.8 respectively.

(a) 100X

(b) 100X

Fig. 4.15 Etched optical micrographs of reduced copper samples sintered at 1273K for 7200 s (a) reduced at 873K (b) reduced at 1073K.

Since difference in initial densities may have affected our conclusions the samples were compacted before sintering so as to have almost similar starting density. The variation of density and relative shrinkage per unit mass for samples reduced at 873K (600°C), 1073K (800°C) and those of atomised copper were cold rolled and then sintering at 1273K (1000°C) show similar behaviour as obtained in sintering of as-reduced samples. Here though the initial densities were same, samples reduced at 873K (600°C) attained a much higher density when sintered for 7200 s (120 min.) than the samples reduced at 1073K (800°C) . This supports the earlier envisaged contention that the enhanced sintering behaviour of copper complacts made by reduction of cuprous oxide preform at 873K (600° C) and 973K (700°C) as against that reduced at 1073K (800°C) is basically due to higher defect concentration introduced in copper phase during reduction and the differences in initial densities of these as-reduced copper compacts do not play a major role during sintering.

CHAPTER- VI

CONCLUSIONS

Conclusions of the present study are

1. The density of coppercompacts obtained from the reduction of cuprous oxide preforms depends upon the reduction temperature. There was relatively less amount of sintering between the neighbouring nucleated and grown islands of copper at a reduction temperature of 873K than 1073K. This resulted into smaller size of conglomerate of nucleated and grown copper islands at 873K reduction temperature than at 1073K.

2. The microstructure of copper compacts produced by the reduction of cuprous oxide at 1073K shows the presence of annealing twins in samples. No annealing twins on the other hand are observed in samples reduced at 873K . These observation suggest that the defects generated during reduction are present in the copper reduced at 873K while they get nearly eliminated when the reduction is carried out at 1073K . Quantitative assessment of defect concentration by X-ray diffraction method could not be made due to the coarsening of grains formed by the sintering between conglomerates of islands at all temperatures.

3. The rate of change of density during sintering at 1273K of copper compacts, obtained from the reduction of cuprous oxide preforms decreases very rapidly upto a

density level of about 3.8 gm/c.c. This is true for all the three copper compacts obtained at reduction temperature studied in the present investigation, viz 873,973 and 1073K. In comparison, the rate of change of density during sintering at 1273K of compacts prepared from the atomized copper powder decreases rather slowly.

4. The sintering behaviour of as-reduced and compacted samples indicate that even though the initial densities are similar copper compacts made by reduction of Cu_2O at 873K sinters faster, a behaviour already observed in sintering of as reduced samples. This supports the contention that enhanced sintering observed in copper compacts reduced at 873K and 973K is basically due to higher defect concentration introduced in copper phase during reduction.

SCOPE FOR FUTURE WORK

1. Methods other than X-ray to find grain size and internal strain in samples with large particle size must be explored.

2. Detailed study of the changes occuring in pore morphology during reduction and sintering can be carried out to get better understanding of the sintering characteristics.

REFERENCES

1. H.H. Hausner, Discussion on the defination of the term ''Sintering'', Sintering-New Developments, Ed. M.M. Ristic, 1977 pp.3-7.

1a. Thumler, as referred in (1).

2. J. White, Basic Phenomena in Sintering, Ceremics Science, Edward Arnold (Publ.) Ltd., 1977, pp.1-19

2a. Pines, as referred in (2).

3. G.C. Kuczynski, Towards the understanding of the process of sintering, Sintering '85, Ed. G.C. Kuczynski, 1985, pp. 3-16.

4. A.S. Reshmawala and G.S. Tendolkar, Powder Metallurgical Review 1, Activated Sintering (Part 1), Powd Met. Int. Vol.1, No.2 , 1969, pp. 58-61.

4a. Genuzin, et.al. as referred in (4).

5. A.J. Shaler, Activated Sintering -A Review, in Sintering and Related Phenomena- 1965, Ed. G.C. Kuczynsl Gorden Breach Science Pbl., 1965, pp. 807-828.

6. M.Eudier, Note on Activated Sintering as influencin the theories of the Sintering Mechanism, ibid, pp. 829-839.

7. W. Schatt and E. Friedrich, Dislocation-Activated Sintering processes, in Sintering '85, Ed., G.C. Kuczynski 1985, pp. 133-141.

8. R. Smoluchowski, as refrred in W.D. Jones, Fundament principles of Powder Metallurgy, Edward Arnold (Pbl. Ltd., 1960, pp.12.

9. F.A. Kroger, Point Defects in Compounds and their Role in Diffusion, Sintering and Related Phenomena, Ed. G.C. Kuczynski, 1965, pp.29-53.

10. E.C. Ellwood and W.A. Weddle, The prduction and properties of oxide-reduced copper powder, J. Inst. Metals, 1951-52, Vol. 80 pp.193-206.

11. W.D. Jones, Manufacture of Metal Powders, Chapter-1, Fundamental Principles of Powder Metallurgy, Edward Arnold Pbls., 1960, pp. 11-14.

12. S. Bhargava and R.K. Dube, Combined Reduction and Sintering of Preformed Cuprous Oxide Strip, Mat Sci. and Tech. Sept. 1985, Vol.1, pp. 743-747.

13. W. Salewski, Measurement of Particle Size and Interna Strain in Doped Tungsten Powder by X-ray Method, Cryst. Res. Technol., Vol. 22, 1987, pp.591-597.

14. S. Bhargava, Preparation and properties of strips made by powder technology route, Ph.D. Thesis, I.I.T. Kanpur 1982.

15. S. Bhargava, Plastic Deformation and Consolidation of Randomly Dense Packed Powder Aggregates: A for - mulation Based on Contact Growth and Lateral Flow in Individual Particles, in press.

16. R. Nicole and A. Rist, The Mechanism of Whisker Growth in the Reduction of Wustite, Met. Trans.B Vol., 10B, 1979 Sept. pp. 429-438.